

THE UNIVERSITY OF MICHIGAN  
INDUSTRY PROGRAM OF THE COLLEGE OF ENGINEERING

ZONE MELTING OF CYCLOHEXANE-RICH  
POLYSTYRENE-CYCLOHEXANE SOLID SOLUTIONS

Arnold M. Ruskin

A dissertation submitted in partial fulfillment  
of the requirements for the degree of  
Doctor of Philosophy in the  
University of Michigan  
Department of Chemical and Metallurgical Engineering  
1962

February, 1962

IP-553

## ACKNOWLEDGMENTS

It is a pleasure for the author to acknowledge the many contributions of others to the research which is the basis of this dissertation.

Professor Giuseppe Parravano, Chairman of the doctoral committee, gave generously of his time and offered suggestions and guidance throughout the course of the research. The other members of the committee, Professors Wilbur C. Bigelow, Edward E. Hucke, Samuel Krimm, Donald R. Mason, and Lawrence H. VanVlack, freely provided constructive criticism, advice and encouragement.

Much help and cooperation was received from fellow graduate students in the Department of Chemical and Metallurgical Engineering. In particular, the author thanks Messers. Fredrick D. Otto, Glen C. Smith, and Phillip P. Spiegelman. Mr. John Wurster, instrument maker, gave considerable help in the design and fabrication of the equipment.

Grateful appreciation is expressed to Dr. H. W. McCormick of the Dow Chemical Company, Midland, Michigan, for providing the polystyrene; to Mr. Theodore F. Beals and the School of Public Health, for use of the ultracentrifuge; and to the Industry Program of the College of Engineering, for the reproduction of this dissertation.

Sincerest thanks are extended to the National Science Foundation for both their Predoctoral Fellowship for the period 1958-1961 and their research grant, administered through the Office of Research Administration.

To all these and many others, the author is indebted  
for invaluable assistance received.

## TABLE OF CONTENTS

	<u>Page</u>
ACKNOWLEDGMENTS.....	ii
LIST OF FIGURES.....	v
LIST OF APPENDICES.....	vii
ABSTRACT.....	viii
INTRODUCTION.....	1
SURVEY OF PREVIOUS WORK.....	3
A. Principles of Zone Melting.....	3
B. Thermodynamic Aspects of Polymeric Systems.....	7
C. Data on Polystyrene-Cyclohexane Systems.....	11
D. Analysis of High Polymer Molecular Weight Distributions.....	12
THEORETICAL CONSIDERATIONS.....	14
EXPERIMENTAL PROCEDURE.....	24
A. Materials.....	24
B. Experimental Methods.....	25
1. Static Tests.....	25
2. Zone Melting Experiments.....	27
RESULTS AND DISCUSSION.....	36
A. Static Tests.....	36
B. Zone Melting Experiments.....	41
1. The Effects of the Number of Zones Passed and of Zone Length.....	41
2. The Effects of Total Polymer Concentration and Zone Travel Rate.....	42
CONCLUSIONS. ....	58
APPENDIX.....	60
BIBLIOGRAPHY.....	79



## LIST OF FIGURES

<u>Figure</u>		<u>Page</u>
1	Concentration of a Solute Species Near a Solid-Liquid Interface.....	5
2	Liquid-Liquid Miscibility Gaps in Binary Systems.....	18
3	Solidification of Binary Systems with Upper Consolute Temperatures.....	20
4	Experimental Arrangement for Obtaining Cooling Curves.....	28
5	Schematic Diagram of the Zone Melting Apparatus.....	30
6	A View of the Zone Melting Apparatus Showing the Heater Supports, Cooling Coils, and Heated Teflon Bearing.....	31
7	A View of the Zone Melting Apparatus Showing the Merry-go-Round in Position.....	32
8	The Sample Tubes on the Merry-go-Round.....	33
9	A View of the Zone Melting Apparatus Showing the Sample Tubes in Position.....	34
10	Ratio of Solute Concentrations in the Solid and Liquid vs. Molecular Weight, Determined by Static Tests on Amorphous Broadly Distributed Polystyrene in Cyclohexane.....	37
11	Ratio of Solute Concentrations in the Solid and Liquid vs. Molecular Weight, Determined by Static Tests on Mixtures of Two Amorphous Narrowly Distributed Polystyrenes in Cyclohexane.....	38
12	Cooling Curves for Cyclohexane-Rich Polystyrene-Cyclohexane Systems.....	40
13	Molecular Weight Distribution Curves of Segments From a Sample of Amorphous Broadly Distributed Polystyrene in Cyclohexane Zone Melted at 4.83 cm./hour.....	43

LIST OF FIGURES CONT'D

<u>Figure</u>		<u>Page</u>
14	Intrinsic Viscosity vs. Sample Position After Zone Melting a Mixture of Two Amorphous Narrowly Distributed Polystyrenes in Cyclohexane at 4.83 cm./hour.....	45
15	Ratio of Solute Concentrations at 1.56 and 2.92 Zone Lengths from the Head End vs. Molecular Weight, Resulting from Zone Melting 0.18 gm./100 cc. Samples at 4.83 cm./hour.....	47
16	Ratio of Solute Concentrations at 1.56 and 2.92 Zone Lengths from the Head End vs. Molecular Weight, Resulting from Zone Melting 0.75 gm./100 cc. Samples at 4.83 cm./hour.....	48
17	Ratio of Solute Concentrations at 1.56 and 2.92 Zone Lengths from the Head End vs. Molecular Weight, Resulting from Zone Melting at 96.6 cm./hour.....	49
18	Ratio of Solute Concentrations at 1.56 and 2.92 Zone Lengths from the Head End vs. Molecular Weight, Resulting from Zone Melting at 4.01 cm./hour.....	50
19	Effective Segregation Coefficient vs. Molecular Weight, Determined by Zone Melting at 4.01 cm./hour..	53
20	Steam-heated, Chrome-plated Steel Ring for Forming Teflon Torroids.....	64
21	Aluminum Plate Used to Maintain Samples Chilled During Their Preparation.....	66

## LIST OF APPENDICES

<u>Appendix</u>	<u>Page</u>
A	ZONE MELTING APPARATUS..... 60
	1. The Shell..... 60
	2. The Electrical Heating System..... 61
	3. The Refrigeration System..... 61
	4. The Motive System..... 61
B	THE FABRICATION AND FILLING OF SAMPLE TUBES..... 63
C	COMPUTER PROGRAM FOR THE SOLUTION OF LORD'S EQUATION FOR THE ZONE MELTED SEMI-INFINITE INGOT IN BENDIX ALGORITHM DECODER LANGUAGE FOR USE ON A BENDIX G-15 COMPUTER..... 67
D	EFFECTIVE SEGREGATION COEFFICIENT VS. THE RATIO OF RESULTING SOLUTE CONCENTRATIONS IN THE ZONE MELTED INGOT AT 1.56 AND 2.92 ZONE LENGTHS FROM THE HEAD END FOR 5 AND 6 ZONES PASSED..... 71
E	A COMPARISON OF POLYMER DIFFUSIONAL VELOCITIES WITH THE RATE OF ZONE TRAVEL IN ZONE MELTING A CYCLO- HEXANE-RICH POLYSTYRENE-CYCLOHEXANE SYSTEM..... 72
F	EXPLANATION AND PRESENTATION OF SEDIMENTATION- VELOCITY DATA FROM WHICH CONCENTRATION RATIOS IN FIGURES 10, 11, 15, 16, 17, AND 18 ARE OBTAINED..... 74
G	SEDIMENTATION-VELOCITY DATA FOR THE FIRST FOUR SEGMENTS OF A POLYSTYRENE-CYCLOHEXANE INGOT WITH AN INITIAL CONCENTRATION OF 2.25 gm/100 cc. ZONE MELTED WITH FIVE 6.35 cm. ZONES PASSED AT 4.83 cm/hr..... 78

## ABSTRACT

The purpose of this investigation is to examine from a fundamental viewpoint the applicability of zone melting to solvent-rich high polymeric systems as a means of achieving a redistribution of the solute species.

Theoretical aspects are considered, and it is concluded that it is necessary to employ a system for which the solution process is endothermic in order to avoid entanglements that would preclude good separations and redistributions. The polystyrene-cyclohexane system meets this criterion and was selected for experimental study.

The experimental procedure includes static solidification tests and zone melting experiments under various operating conditions. Distribution analyses are performed by ultracentrifuge sedimentation-velocity methods.

It has been found on slow zone travel rates (ca. 4.01 cm/hour) that redistribution of polystyrene across the advancing freezing interface of a cyclohexane-rich polystyrene-cyclohexane system tends toward accumulating all polymer species at the first-frozen part of the ingot. The effect is largest for the highest molecular weight species. At faster zone travel rates (ca. 4.83 cm/hour), resorption of a polymer-rich second phase in the liquid is comparatively too slow to permit equilibrium to be reached, and this phase is carried in the moving liquid zone. The higher molecular weight species are particularly

susceptible to this effect, and are preferentially accumulated in the last-frozen part of the ingot. Increases in total polymer concentrations and in the proportion of high molecular weight species enhance the latter effect at all rates of zone travel. Extremely rapid rates of zone travel. (ca. 9.66 cm/hour) result in very little redistribution of the solute species because of their relatively low mobility compared to the rate of advance of the freezing interface.

For an initially broadly distributed polymer, in no case can a single species be localized by zone melting a dilutely concentrated ingot without the presence of considerable quantities of slightly smaller and slightly larger molecules. However, proper choice of the total polymer concentration and rate of zone travel can allow rough separations to be effected; suitable combinations of successive zone melting operations may permit a moderate degree of fractionation to be achieved.

## INTRODUCTION

The term "zone melting" refers to an automated method for accumulating the effects of successive fractional crystallizations on the distribution of solute species.<sup>(25)</sup> A short molten zone is passed through a solid solution, and as the freezing interface progresses, there is a continual redistribution of the various solute species according to their relative solubilities in the liquid and solid phases. If diffusion of solutes does not occur in the solid but does occur in the liquid, a concentration gradient is developed over the length of the resulting solid ingot. Passing successive molten zones through the ingot results in accumulating the segregation effects. This method, in its many variations, has been effectively employed to localize solute species in alloy systems. Because the various members of a structurally homologous series exhibit a range of properties, the generality of the technique suggests that it could perhaps be extended to effect a redistribution of dissolved polymer species in a frozen solvent. Successful application of zone melting to high polymeric systems would permit more economical large scale separations attractive both as an industrial tool and as a means of concentrating selected species for use in research investigations. With an eye toward the applications of the method, some cursory experiments have been reported. Nowhere, though, has mention been made of investigating the effect of operating variables on the distribution of resulting properties for each segment of the zone melted ingot.

In view of the importance of these types of data, it was decided to develop suitable equipment for studying zone melting of dilute solutions of high polymers and then to obtain specific information on a representative material. For the latter, polystyrene was selected, and the majority of the work reported herein concerns the polystyrene-cyclohexane system.

## SURVEY OF PREVIOUS WORK

A few investigators have reported measurements of single properties, e.g. intrinsic viscosity or melting point, of paraffins and high polymers subjected to zone melting. Peaker and Robb<sup>(22)</sup> report redistributing poly-disperse polystyrene in naphthalene. Eldib<sup>(7)</sup> has zone melted mixtures of paraffinic waxes. Cahill and Loconti<sup>(4)</sup> have reported the results of unidirectional freezing of polystyrene-benzene solutions which they performed preliminary to zone-fractionation studies. Their results show that some redistribution does indeed occur during the process: the appropriate averages or extreme values of the property measured varied systematically along the zone melted ingot. However, these references include no indication of the distribution of properties within each segment of the zone melted ingot.

Although the lack of specific information on zone melting of polymer systems is significant, there is no lack of general, background considerations pertinent to the topic. These include principles of zone melting, thermodynamic aspects of polymeric systems, and data available on the system polystyrene-cyclohexane. In addition there is work in supporting fields such as analysis of high polymer molecular weight distributions. Each of these will be discussed in turn.

### Principles of Zone Melting

The principles of zone melting were first mentioned by Pfann in 1952,<sup>(24)</sup> who has since excellently reviewed many of the important



developments pertaining to elemental systems in a monograph.<sup>(25)</sup>

There are two mathematical treatments of the zone melting operation - that are incidentally referred to by Pfann<sup>(25)</sup> - which can be mentioned in some detail. Burton et al.<sup>(3)</sup> considered the advance of a freezing interface into a liquid at a finite rate. Under this condition, a concentration gradient will be developed instantaneously in the liquid phase as a result of the solid either rejecting into the liquid or removing from the liquid the solute species. This effect is shown schematically in Figure 1, where Figure 1a represents the case of the solid rejecting the solute, and Figure 1b the case of the solid depleting the liquid of solute. To the extent that diffusion in the liquid is not instantaneous and not capable of immediately reducing the gradient, the ratio of concentration of solute in the solid to that in the liquid will vary as a function of liquid position. The value of this ratio at the interface corresponds to the equilibrium phase diagram, and is known as the equilibrium segregation coefficient. The value of the ratio at a position in the bulk liquid away from the boundary layer is the one which controls the efficacy of the zone melting operation, and is known as the effective segregation coefficient. By means of a mass balance Burton showed that the two values of the segregation coefficient could be related in terms of the rate of advance of the freezing interface,  $f$ , the thickness of the boundary layer  $\delta$ , and the solute's diffusion coefficient,  $D$ :

$$\ln \left( \frac{1}{K_{\text{eff}}} - 1 \right) = \ln \left( \frac{1}{K_{\text{equil}}} - 1 \right) - \frac{f\delta}{D}$$

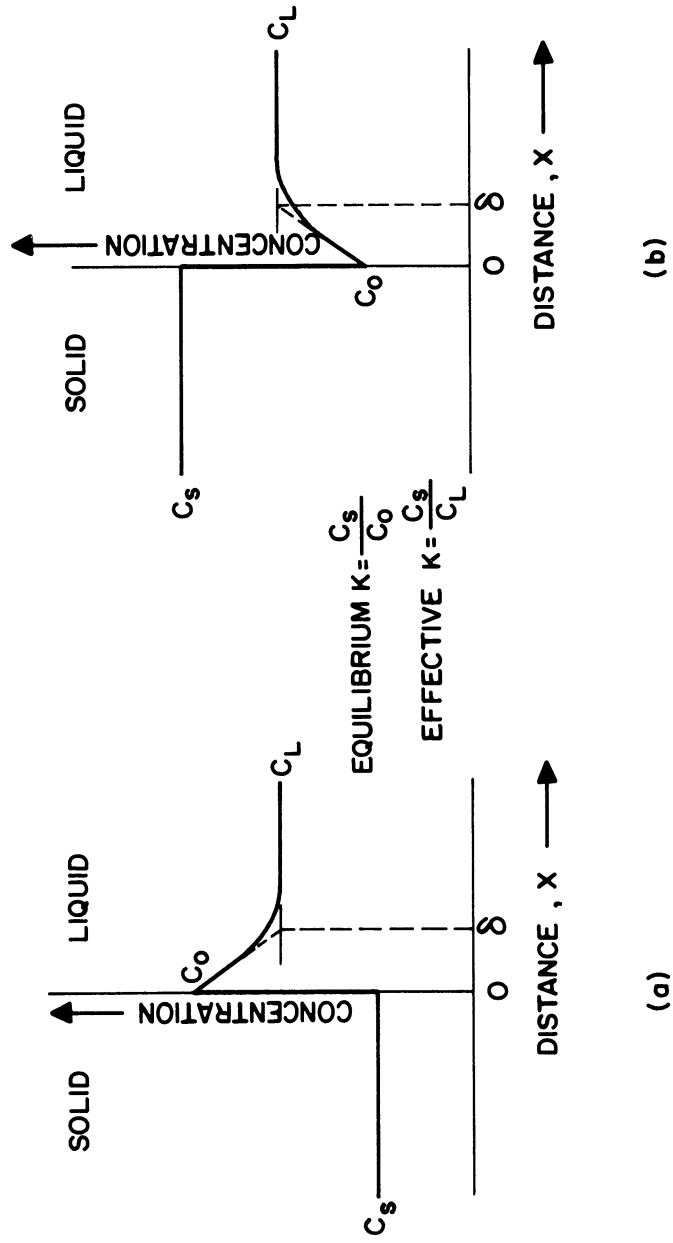


Figure 1. Concentration of a Solute Species Near a Solid-Liquid Interface.  
(a) The Solid Rejects Solute into the Liquid.  
(b) The Solid Retains Solute from the Liquid.

$$\text{for } K_{\text{equil}} = \frac{\text{CONC}_{\text{solid}}}{\text{CONC}_{\text{liquid}}} \Bigg|_{\text{interface}} < 1$$

$$\text{or } \ln \left( 1 - \frac{1}{K_{\text{eff}}} \right) = \ln \left( 1 - \frac{1}{K_{\text{equil}}} \right) - \frac{f\delta}{D}$$

$$\text{for } K_{\text{equil}} = \frac{\text{CONC}_{\text{solid}}}{\text{CONC}_{\text{liquid}}} \Bigg|_{\text{interface}} > 1$$

It should be noted at this point that for  $K_{\text{equil}}$  greater than 1.0,  $K_{\text{eff}}$  will always be greater than 1.0; and for  $K_{\text{equil}}$  less than 1.0  $K_{\text{eff}}$  will always be less than 1.0.

In 1953, Lord<sup>(15)</sup> showed that a differential equation describing the effects of passing one molten zone through a semi-infinite ingot in terms of the effective segregation coefficient and the position in the ingot could be solved reiteratively to yield a compact expression describing the net effect after several passes:

$$C_n(a) = C_o \left\{ 1 - [(1-K)e^{-Ka}] \left[ n - \sum_{t=1}^{n-1} \sum_{s=1}^t K^{s-1} e^{-sK} \sum_{r=0}^{s-1} \frac{s^{s-r-2} a^r (r+1 - Ka)}{(s-r-1)! r!} \right] \right\}$$

where  $C$  is the solute concentration,

$K$  is the effective segregation coefficient,

$n$  is the number of zones passed,

$a$  is the distance in the ingot from the head end measured in zone lengths,

When it is applied to finite ingots, Lord's expression correctly describes only as much of the ingot as is not subject to realizing that normal freezing\* occurs at the tail end. On the first pass, only the

\* "Normal freezing" refers to solidification of a liquid with no influx of additional liquid during the process.

last zone length experiences normal freezing. On the second pass, the next to last zone length will incorporate in the liquid some of the material that was previously frozen normally in the last zone length and this effect will be felt at the freezing interface at the beginning and throughout the next-to-last zone length; the last zone length itself will again freeze normally. On the third pass, the third zone length from the end will similarly incorporate the effects of the first normal freezing that were transferred to the second zone length on the second pass. And the second zone length will again be affected by the normal freezing in the last zone. The effect of normal freezing is thus transferred backwards one zone length more upon the passing of one additional zone. The applicable part is therefore all of the ingot except a length equal to the number of zones passed times one zone length. Other limitations on the application of the expression are that the zone length must be the same on each pass, and that the effective segregation coefficient must be relatively constant over the range of concentrations that exist in the zone melting operation.

#### Thermodynamic Aspects of Polymeric Systems

Thermodynamic considerations of polymeric systems have been made both theoretically and experimentally. Theoretical approaches have centered on computing phase equilibria by examining chemical potentials for the various members of a polydisperse polymer or for the solvent in a polymer-solvent system.<sup>(8)</sup> Regardless of their amount of sophistication, the theories are all characterized by equating the entropy of mixing with the entropy of configuration. Deviations from

this relation have, by and large, been absorbed in heat of mixing terms. The configurational entropy is based on segments of the polymer chain - in contradistinction to ideal solution theories which are based on whole molecules. The heat of mixing is similarly computed on the basis of a heat effect per unit contact of a polymer molecule segment with a solvent molecule. (8,27,31)

In the computation of configurational entropies, an arbitrary liquid lattice is assumed, and the various segments of polymer molecules and the solvent molecules are placed on the lattice in manners consistent with the fact that contiguous polymer segments must be put on adjacent lattice sites. The configurational entropy is then computed from the Boltzman expression where it is proportional to the natural logarithm of the total number of distinguishable ways that the components of the solution can be arranged.

Two limiting cases are recognized for this computation. (8,27) On one hand, the solution is sufficiently concentrated that even if the polymer molecules are more-or-less coiled up, an arbitrarily chosen polymer segment views an essentially spatially homogeneous distribution of segments and solvent molecules. The resulting expression<sup>(8)</sup> for the total entropy in this case is

$$\Delta S = -k \left( \sum_i n_i \ln v_i \right)$$

where  $n_i$  refers to the number of molecules and  $v_i$  refers to the volume fraction of the molecules. One of the species is the solvent; all others are polymer molecules of various character.

The other extreme can occur when the polymer molecules prefer themselves to the solvent as neighbors and coil up. Then if the solution is sufficiently dilute, the presence of coiled molecules leaves a sizeable fraction of the solution with no polymer segments, and a molecule outside the solution sees two distinctly different regions. In the region of the solution where the segment concentration is appreciable, theoretical considerations give chemical potential expressions corresponding to those pertinent to the entire moderately concentrated solution. In the regions where there are no solute species, the expressions for configurational entropy are clearly those for pure solvent.<sup>(8)</sup> Thus, although it is possible to write a weighted expression for the solvent under these conditions, there is for the various solute species apparently no straightforward way of expressing their configurational entropy so that this case could be distinguished from the more concentrated situations.<sup>(8)</sup>

Various authors<sup>(9,11,21)</sup> have attempted to take into account the existence of interactions which bias the probability of some of the possible configurations. It has generally been acknowledged<sup>(8)</sup> that these approaches add little to the overall agreement between theory and experiment. Thus, in order to preserve the simplicity of the form of the non-biased expressions, these terms are generally omitted, and any error their omission introduces into the subsequent expressions for the chemical potential is absorbed in the heat of mixing term.

Heats of mixing<sup>(8,31)</sup> are of the type wherein a suitable average number of contacts between unlike pairs of solvent molecules and polymer segments is used to estimate the interaction energy. As noted above, the experimental value of this term will include contributions arising from specific spatial interactions, as well as simple unlike-pair interactions. Generally, the form of this term is simply

$$\Delta H = z(\Delta w_{12}) n_1 v_2$$

where  $z$  is the number of unlike contacts per chain segment (usually 3 or 4),  $(\Delta w_{12})$  is the net exchange energy per contact,  $n_1$  is the number of solvent molecules, and  $v_2$  is the site or volume fraction of the polymer. By equating  $\chi_1$  to  $\frac{z\Delta w_{12}}{kT}$ , the form

$$\Delta H = \chi_1 kT n_1 v_2$$

can be given, which puts the measured product of uncertain quantities as a multiple of  $kT$ .

The resulting Gibbs' free energy can be written as

$$\Delta G = kT \left[ \sum_i n_i \ln v_i + \chi_1 n_1 v_2 \right]$$

where  $v_2 = \sum_{i=1} v_i$ .

After changing to a mol basis, partial differentiation with respect to  $n_1$  gives after some manipulation the partial molar free energy or chemical potential. Thus, the chemical potential can be written

$$\mu_i - \mu_i^0 = RT \left[ \ln v_i - (x_i - 1) + v_2 x_i \left( 1 - \frac{1}{x_n} \right) + \chi_1 x_i (1 - v_2)^2 \right].$$

where  $\mu_i$  is the chemical potential,  $x_i$  is the chain length (no. of segments) of chain  $i$ , and  $x_n$  is the number average molecular weight for the total polymer in the phase in question.

At equilibrium between two phases, the chemical potential for species  $i$  in the two phases will be equal. From this relation the ratio of volume fractions for the species in the two phases designated as primed ( $'$ ) and unprimed, i.e. the equilibrium segregation coefficient, can be written

$$\frac{v_i'}{v_i} = K_{\text{equil}} = \exp \left\{ (x_i) \left( v_2 \left( 1 - \frac{1}{x_n} \right) - v_2' \left( 1 - \frac{1}{x_n'} \right) + \chi_1 [(1 - v_2)^2 - (1 - v_2')^2] \right) \right\}.$$

Attempts to experimentally verify the above theory have taken many forms. Early investigations took the form of liquid-liquid equilibria, and they are well summarized by Flory.<sup>(8)</sup> More recently, the theories have been extended to systems involving the crystallization of polymers where the partition is between the polymer crystal and either a liquid solution or an amorphous region of polymer.<sup>(9)\*</sup> Generally, it can be said of both kinds of investigations that the theory is of the proper form. Deviations can be ascribed to non-constancy of various parameters, e.g.  $\chi_1$ , that have been assumed constant over various operating conditions.

#### Data On Polystyrene-Cyclohexane Systems

Data on the polystyrene-cyclohexane system in the liquid phase have been available for many years. Fox and Flory<sup>(10)</sup> have reported values on thermodynamic interaction parameters, and have

---

\* It should be noted that a lack of a thorough understanding of the kinetics of crystallization of polymers has hindered the interpretation of the thermodynamic aspects. As a result, the most recent efforts have centered on the mechanisms of crystallization, with little new work being done in thermodynamic investigations.



shown the following results: In cyclohexane, polystyrene is only partially miscible at certain temperatures. The maximum temperature at which a precipitate is stable has a minimum at low concentrations of polymer and then increases with increasing volume fraction of polymer for a polymer of a given (narrowly distributed) molecular weight. The critical or maximum precipitation temperature varies directly with the square root of the molecular weight. The intrinsic viscosity varies directly with the concentration of a polymer species, and the first derivative of the relation increases with increasing molecular weight. Variations with temperature of chain dimensions, as measured by the root mean square end-to-end distance, are slight over a range encompassing both sides of the miscibility gap.

#### Analysis of High Polymer Molecular Weight Distributions

In addition to background considerations pertinent to zone melting of high polymers, there has been developed a body of literature pertaining to the analysis of high polymer distributions. Traditionally, distribution analyses have been performed by examining number-average, viscosity-average, or weight-average molecular weights of the fractions from carefully fractionated samples.<sup>(8)</sup> These values were obtained from osmometry, viscometry, or light scattering experiments, respectively. Fractionation was accomplished by altering the volumes and temperatures of liquid-liquid systems, according to the partition theory indicated above. In recent years, techniques such as gradient-elution experiments<sup>(6)</sup> and counter-current liquid-liquid extraction<sup>(1)</sup> and thermal diffusion<sup>(14)</sup> have been attempted as fractionation tools, but the

analyses of the fractions have remained the same. Finally, techniques employing the ultracentrifuge<sup>(28,29)</sup> have been developed which allow the determination of molecular weight distributions of unfractionated polymer samples. The entire range of the applicability of the ultracentrifuge to high polymers is reviewed by Baldwin and Van Holde,<sup>(2)</sup> and the determination of molecular weight distributions of polystyrene using the instrument is reported by McCormick<sup>(17)</sup> and Cantow.<sup>(5)</sup>

## THEORETICAL CONSIDERATIONS

Zone melting, or even the simpler process, fractional crystallization, succeeds because different solute concentrations coexist in the liquid and solid phases at equilibrium at temperatures in the solidification temperature range. For many kinds of systems, information about these concentrations abounds, and is conveniently and commonly presented in equilibrium diagrams. In the case of polymer-solvent systems, however, there can be found no reports of phase equilibria for temperatures approaching the solidification range. In the absence of detailed knowledge about the phase equilibria for any polymer-solvent system under the conditions pertaining in zone melting, it is necessary to consider some general, theoretical aspects of thermodynamics in order to anticipate the results of the operation.

Based on equilibrium studies of amorphous polymer-solvent systems wholly in the liquid region,<sup>(26)</sup> it can be said that in reality only two kinds of systems are encountered: (a) systems which possess only a single-phase liquid region over all temperatures regardless of the concentration of the polymer in the solvent, and (b) systems in which for some concentrations of the polymer in the solvent, there is a two-liquid region formed, indicating a miscibility gap, at least over certain temperatures. It should be noted that for the purposes of the entire discussion that follows, amorphous polymers are considered liquids; this definition is convenient and simplifies the discussion, but it is not a necessary restriction.

The first situation is one for which the solution process is exothermic and which results in the polymer molecules uncoiling to expose themselves to as much solvent as possible. Flory has shown that in a thermodynamically good solvent the excluded volume of two

identical spheres of polymer is eight times the volume of either sphere alone.<sup>(8)</sup> He has also shown that the root-mean-square end-to-end distance in a good solvent may be up to twice as long as it is in a poor solvent.<sup>(8)</sup> Thus, the effective volume of a polymer in a good solvent may approach 16 times what would be calculated on the basis of its specific volume as a pure component. As a result, at weight concentrations of polymer of only a few per cent, its effective volume fraction in a good solvent may be appreciable, and at moderate concentrations, it is very significant. There is consequently considerable opportunity for spatial or mechanical interlocking if the weight fractions of polymers in good solvents are just a few percent.

In the second case, the solution process is endothermic and results in the individual polymer molecules remaining tightly coiled in order to have as little contact with the solvent as possible. In this situation polymer-polymer molecular interactions are reduced to a minimum.

Polymer-polymer molecular entanglements, that may exist when the solution process is exothermic, cause unselective entrapment of the polymer molecules on freezing of the system. The first polymer species incorporated into the solid mechanically retain other species which are then engulfed by the advancing freezing interface. As a result of the strong tendency toward unselective entrapments, efficient redistribution on freezing of a system with a solvent that is thermodynamically good at temperatures just above the solidification temperature range is precluded at all but the very lowest concentrations.

In the case of minimal polymer-polymer molecular interactions, which obtains when the solution process is endothermic, each polymer molecule "sees" only the solvent. The solvent, to be sure, sees the effect of all the polymer molecules. When dynamic equilibrium of the polymer molecules is being established across a phase boundary, however, each polymer molecule in turn weighs the advantages of locating in each of the two phases. Upon a molecule's selecting one phase or the other, the population situation for the phases is changed, and the next molecule's decision will be influenced by this subtle change. The process will continue, with phase populations oscillating over time with diminishing amplitudes until a steady-state situation is reached. It is obvious from this description that the total polymer concentration and molecular weight distribution will influence the partition of any selected species across a phase boundary, and this is also confirmed by the solution lattice theories (see the previous chapter). Thus, a polydisperse polymer-solvent system that exhibits an endothermic solution process can be considered as a family of a series of binary systems where the series parameter is molecular weight and the family parameters are total polymer concentration and molecular weight distribution. Appropriate binary equilibrium diagrams should then provide the information desired to anticipate the results of zone melting experiments.

Unfortunately, not even the binary diagrams exist, and a further attempt must be made to secure the needed information. This can be accomplished by considering the limited number of possibilities

available in binary systems with liquid-liquid miscibility gaps and then performing critical experiments to distinguish which kind of situation really exists.

For binary systems there are only three kinds of equilibrium diagrams possible for liquid regions with miscibility gaps.<sup>(18)</sup> These are shown in Figure 2. Figure 2a depicts an upper consolute temperature where two liquid phases coexist at lower temperatures, but at temperatures greater than the consolute temperature, only one liquid phase exists. In Figure 2b is shown a system which possesses a single liquid phase at lower temperatures, but which changes to a two-liquid region at higher temperatures. In Figure 2c is shown a system demonstrating an upper consolute temperature and a lower consolute temperature. Both of the cases with lower consolute temperatures possess single phase liquids as the temperature decreases toward the freezing point. Therefore, although at some temperatures there is a miscibility gap, the gap does not extend to temperatures just above the solidification range. As a result, for the latter cases when the solute species are polymer molecules, they do not exist free of entanglement (at all concentrations except the very lowest) and thereby are subject to the same unselective entrapment on freezing that polymer molecules in wholly single phase liquid regions experience. Thus, only the first case (the upper consolute temperature) needs to be considered in greater detail.

On the basis of the phase rule of Gibbs, for a binary system at constant pressure the maximum number of phases that can exist is three, which can only happen when the temperature is invariant. Two

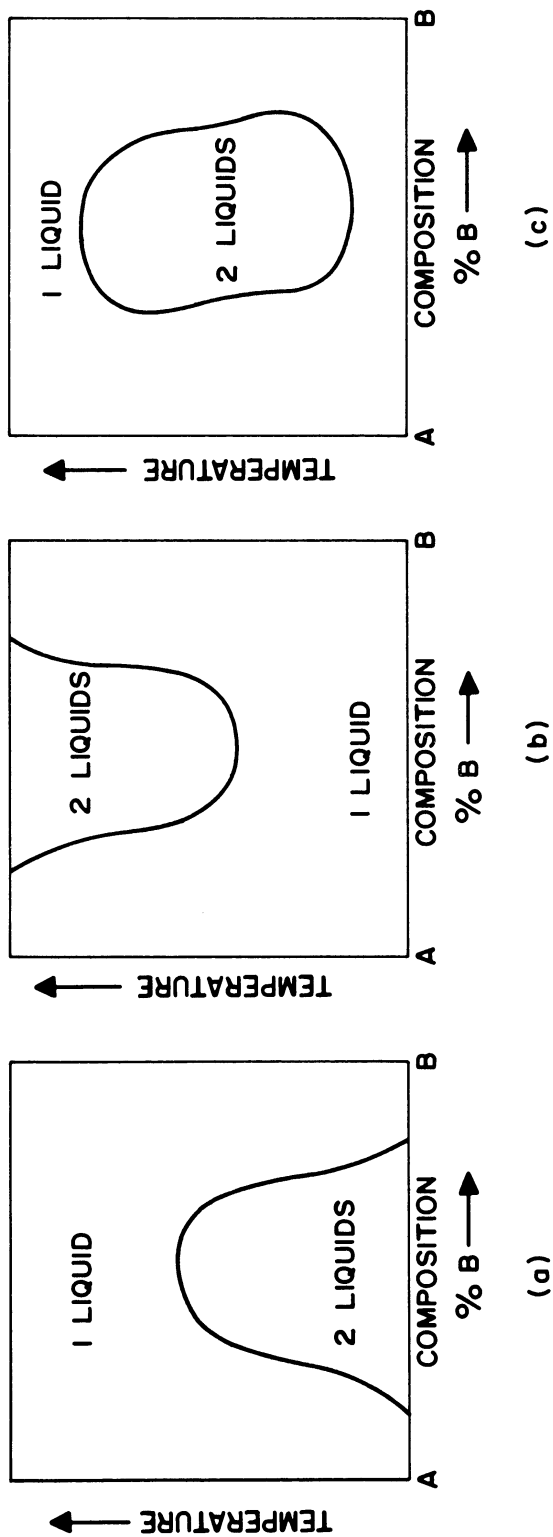


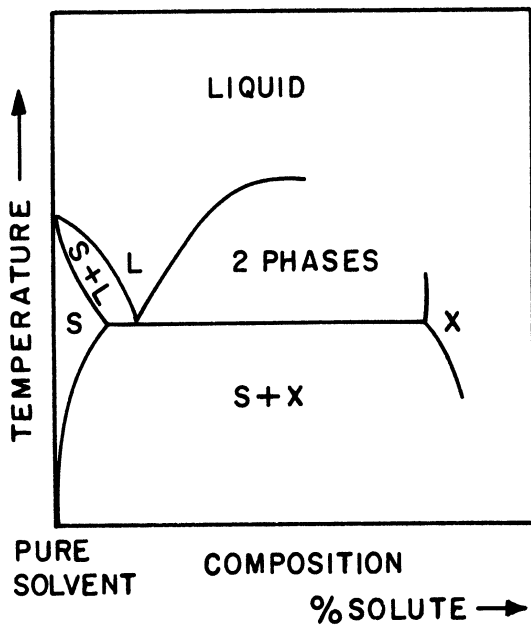
Figure 2. Liquid-Liquid Miscibility Gaps in Binary Systems.  
(a) Upper Consolute Temperature  
(b) Lower Consolute Temperature  
(c) Upper and Lower Consolute Temperatures.

phases, the two liquids, have already been established for the case at hand. Therefore, upon wishing to examine the situation of freezing, the third and final phase present is set as the solid. It is a well-known fact that when three phases coexist in a binary system at constant pressure and one of the three phases is one of the pure component solids with some of the second component dissolved in it, the invariant temperature cannot be the melting point of the first pure component. Hence, the invariant temperature must be either above or below the melting point of the pure component solvent.

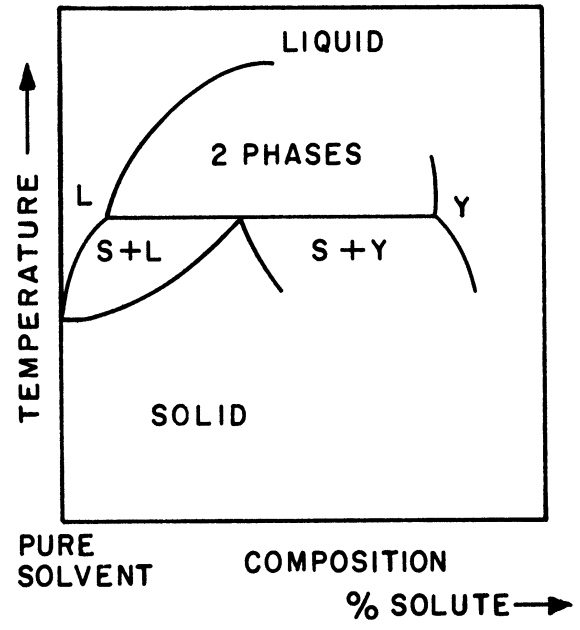
Figure 3 presents the two alternatives that remain which are pertinent to zone melting of polymer-solvent systems. Figure 3a shows the case where the two phase liquid region terminates on cooling at a temperature below the pure component melting point, and Figure 3b shows the case where the invariant temperature is above the pure component melting point. In the former case, the solute concentration is greater in the liquid than in the solid for any given temperature. In the latter case, the relative concentrations are reversed.

If a polymer-solvent system displaying either one or the other of these characteristics is subjected to zone melting under conditions where thermodynamic equilibrium is essentially reached, the following conclusions can be made. If the invariant temperature is greater than the pure solvent melting point, then zone melting will result in the solute being concentrated at the head (i.e. the first melted and the first frozen) end of the ingot. But if the





(a)



(b)

Figure 3. Solidification of Binary Systems with Upper Consolute Temperatures.

- (a) Pure Solvent Melting Point Above Solidus Temperature.
- (b) Pure Solvent Melting Point Below Solidus Temperature.

invariant temperature is below the pure solvent melting point, the solute will remain preferentially in the liquid and be carried to the tail (i.e. the last frozen) end of the ingot.

The previous discussion pertains to zone melting suitable polymer-solvent systems under conditions where thermodynamic equilibrium is approached. However, the fact that in zone melting freezing occurs at a finite rate introduces the element of time, and thermodynamic equilibrium may not be obtained.

Time-dependent deviations from thermodynamic equilibrium can be of two kinds. One kind of deviation is due to finite diffusion rates in the liquid and results in less net segregation between the liquid and solid than thermodynamics would predict. This situation has been described in some detail in the previous chapter.

The second kind of time-dependent deviation is the result of the finite rates at which three-phase reactions occur. The situation becomes important only if the reaction rate is slow compared to the rate of advance of the freezing interface. Two cases can be distinguished here, according to the relation between the invariant temperature and the melting point of the pure solvent.

When the invariant temperature is above the pure solvent's melting point, the two liquids must react to form the solid. One of the liquids is largely polymer, and if the reaction is too slow, a polymer-rich phase remains after solidification. The remaining polymer may either be entrapped in the freezing solid, or be pushed along in the liquid by the advancing interface. Since the larger

polymer molecules are more stable as second-phase material than the smaller ones,<sup>(8)</sup> if entrapment occurs in addition to the thermodynamic tendency for the larger molecules to be retained in the solid, total retention of the larger molecules in the solid will be enhanced. But if pushing into the liquid of the more stable second-phase larger molecules occurs, the net effect will be less than the thermodynamic retention of larger polymer molecules by the solid.

When the invariant temperature is below the pure solvent's melting point, the solvent-rich liquid reacts to form solvent-rich solid and polymer-rich liquid. This polymer-rich liquid is in addition to any polymer-rich liquid already present. In this case, as in the case above, the polymer-rich liquid can either be entrapped or pushed ahead. However, entrapment works against the thermodynamic tendency in this case where the polymer should be rejected into the liquid, and pushing ahead enhances the thermodynamic tendency.

It is now possible to outline what steps are necessary to be able to anticipate the results of zone melting a polymer-solvent system when a suitable miscibility gap exists in the liquid region. For each species, either the relative concentrations of solute in the liquid and the solid must be determined, or the invariant temperatures must be known relative to the pure solvent melting temperature. This task is not as formidable as it seems, for an examination of the solution lattice theory, given in the previous chapter, shows that the coefficient of the chain length in the expression for the logarithm of the relative concentrations of one species across two phases does not change algebraic sign with a variation in chain length. Therefore, it suffices

to measure the partition tendency for only a single molecular species in the solvent at solidification in order to determine the tendency for all members of a structurally homologous series. Then zone melting can be carried out at different rates of zone travel and the net partition assessed.

## EXPERIMENTAL PROCEDURE

### Materials

Polystyrene was selected for study because of its ready availability in a range of molecular weight distributions and because considerable work has been reported on its characterization<sup>(5,10,17)</sup> Both a broadly distributed and two narrowly distributed amorphous polymers have been examined.

The more broadly distributed material was found to have a weight-average molecular weight of 243,000 as determined by the ultracentrifuge sedimentation-velocity method of McCormick<sup>(17)</sup> and 295,000 similar to that observed by other authors.<sup>(12,13)</sup> A ratio of weight-average to number average molecular weight of 2.055<sup>(16)</sup> was determined by the turbidity titration method of Morey and Tamblyn.<sup>(19)</sup>

The two narrowly distributed amorphous polymers have weight average molecular weights of 82,000 and 267,000. The former had a weight-average to number-average molecular weight ratio of 1.05,<sup>(16)</sup> whereas the same ratio for the latter was found to be 1.08.<sup>(16)</sup> These values were determined by ultracentrifuge sedimentation-velocity experiments.

Selection of an appropriate solvent was based on three factors: (a) the desirability for the solvent-polymer system being thermodynamically poor (i.e. have an endothermic heat of solution), so that there would be considerable likelihood that the polymer molecules would remain individually tightly coiled and give rise to a minimum of polymer-polymer

interactions; (b) the availability of well-documented methods of characterization of polystyrene in the solvent selected, so that transfer of the polymer from one solvent to another could be avoided in order to avoid an additional redistribution of solute species that would accompany such a transfer; and (c) the resulting system's range of freezing temperature being within a range that could be handled with equipment that could be developed.

On basis of the first two factors, cyclohexane was considered, <sup>(23,24)</sup> and a check of the third factor proved that the range of freezing temperatures would be in the vicinity of 0°C. Thus, the system polystyrene-cyclohexane was chosen for the more detailed study.

Solutions of the desired concentrations were prepared by dissolving the polystyrene in the cyclohexane at temperatures near the boiling point of the solvent (81°C).

## Experimental Methods

### Static Tests

In order to be able to anticipate the results of zone-melting cyclohexane-rich polystyrene-cyclohexane systems, it was necessary to ascertain the thermodynamic tendency for partition of the polystyrene molecules across the freezing interface. For this purpose, a series of static tests was performed.

Test tubes 20 mm.O.D. by 150 mm. long were supported with their lower third in an ice water bath and filled approximately two-thirds full. After periods of 120 minutes or 160 minutes, the supernatant liquids were decanted and the solids remaining were allowed to melt. The melted solutions were recovered after being heated into the temperature range above

any critical temperatures. The molecular weight distributions of the various fractions were determined with the use of a Spinco Model E Ultracentrifuge via sedimentation velocity experiments according to the methods of McCormick<sup>(17)</sup> and Cantow.<sup>(5)</sup> Runs were made in cyclohexane at the  $\theta$ -temperature, 35°C, at concentrations between 0.10 and 0.20 gm./100 cc. All runs were made at 59,780 r.p.m. with a double sector cell. Boundary curves were measured by projecting them onto co-ordinate paper. Diffusion corrections were made by extrapolating against  $1/t$  to infinite time.<sup>(5,17)</sup> Corrections for concentration at this level of concentration were found to be unnecessary (see also reference 16). Because there was no detectable differences between the 120 minute and the 160 minute samples, longer times were deemed unnecessary.

In an attempt to determine whether there might be significant entrapment in the experiment just described, 90 mm. watch glasses in point contact with the ice water bath were substituted for the test tubes. In order to reduce the amount of solvent evaporation from the large amount of exposed surface, inverted watch glasses were used as covers. In no case, however, was it possible to maintain a liquid above some solid: holding the entire, shallow assembly at the equilibrium freezing temperature was not possible, and growth of the solid soon consumed the entire system. It was noticed during the watch glass experiment, however, that the second phase occurring in the liquid - mentioned in the preceding chapter - was definitely observable to the naked eye and was largely particulate. A piece of the frozen solution was slowly moved in the vicinity of the second phase particles with a pair of tweezers to qualitatively determine the extent of attraction of the solid for the second phase.

A further indication of the true partition tendency was sought by obtaining cooling curve data which would show whether the liquidus temperature for the solution was higher or lower than the melting point of the pure solvent. Special pains were exercised to avoid either constitutional supercooling or thermal undercooling, by using the arrangement sketched in Figure 4 and by stirring and tapping the sample tube. By this technique, the rate of heat extraction was made very slow and nucleation was enhanced, resulting in precision closer than 0.1 centigrade degree.

#### Zone Melting Experiments

Carefully controlled movement of a molten zone through a solid ingot of a cyclohexane-rich polystyrene-cyclohexane system necessitates a suitable heat sink at temperatures considerably below 0°C in order to maintain well-defined liquid-solid interfaces. The use of such temperatures as ambient conditions for a mechanical system, however, creates operational difficulties not common to more conventional applications of zone melting. As a result, an apparatus had to be developed to take into consideration such items as the development of ice in bearings and mechanical drives, the necessity of reducing the amount of surface of the apparatus to reduce the heat influx through the insulation, and the necessity for having rigid cooling coils in close proximity to the zone melted sample.

These design considerations dictated that the sample should be moved as simply as possible past fixed local heaters in a refrigerated volume, and that a circular rather than a longitudinal motion was



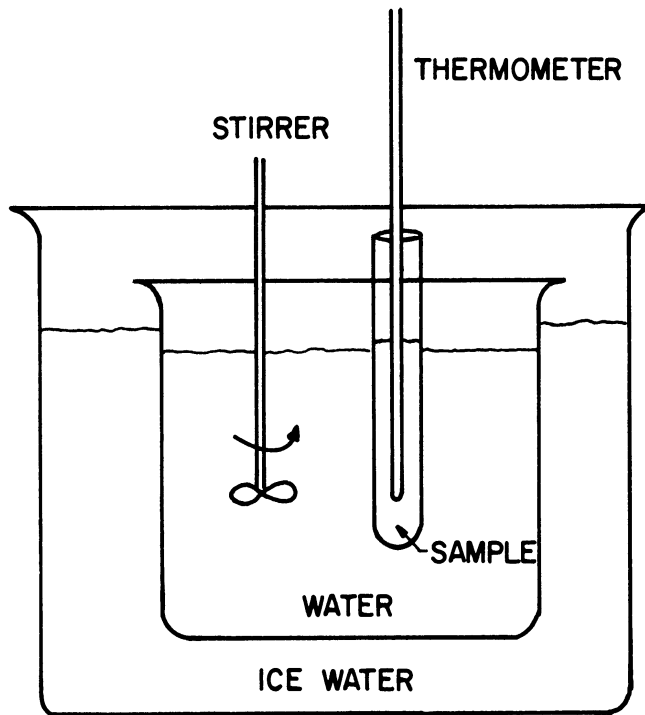


Figure 4. Experimental Arrangement for Obtaining Cooling Curves.

to be preferred. The arrangement used consisted of toroid-shaped samples being carried in Teflon tubes on a merry-go-round past radiant heaters in a 62cm. square box maintained at  $-30^{\circ}\text{C}$  by a refrigerating unit. The set-up is shown in Figure 5, a schematic diagram, and in the several photographs that follow. Specific information regarding the construction of the equipment and the fabrication and filling of sample tubes is given in the Appendix.

By slowly rotating the merry-go-round, successive parts of the samples are brought in front of the heater for local melting. As the part of the sample in front of the heater is removed from this vicinity, the ambient conditions induce freezing, and the accompanying redistribution of solutes. Successive passing of the molten zone through the ingot enhances the net redistribution of solutes until an ultimate distribution is approached.

Molten zones of 4.44 or 6.35 cm. lengths were passed at the rate of 9.66, 4.83 or 4.01 cm. per hour through 96.6 cm. long by 1.15 cm. diameter samples of initial total polymer concentrations ranging from 0.18 to 1.30 gm./100 cc. The shorter zone length represents the lower limit on the zone size that could be maintained with all values of concentration and speed of rotation examined. The longer length represents a suitable differential in zone size for the examination of the effect of zone size in this range. Matter transport<sup>(25)</sup> was prevented by completely filling the sample containers initially.

Samples were recovered from the zone melted ingots by cutting them with a high speed saw into short sections which were

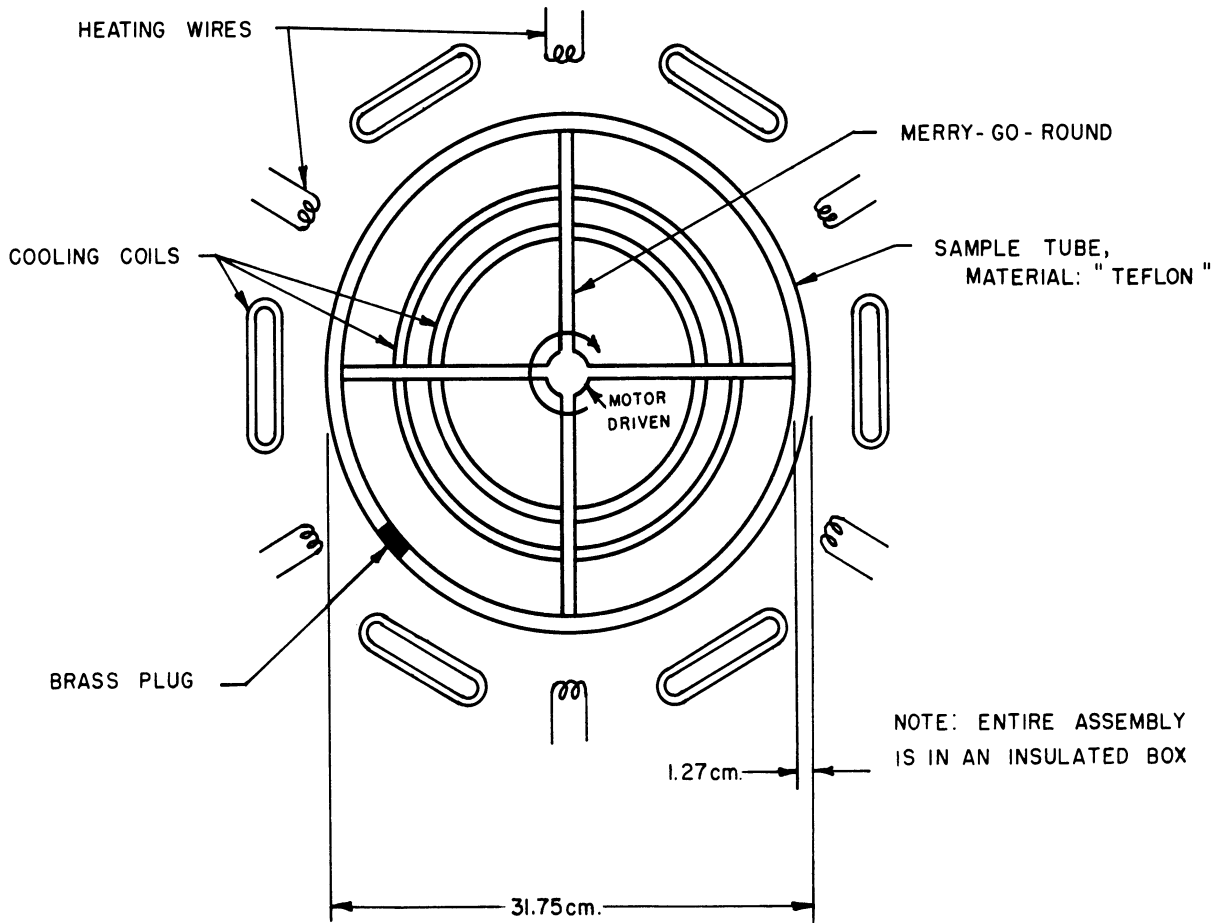


Figure 5. Schematic Diagram of the Zone Melting Apparatus.

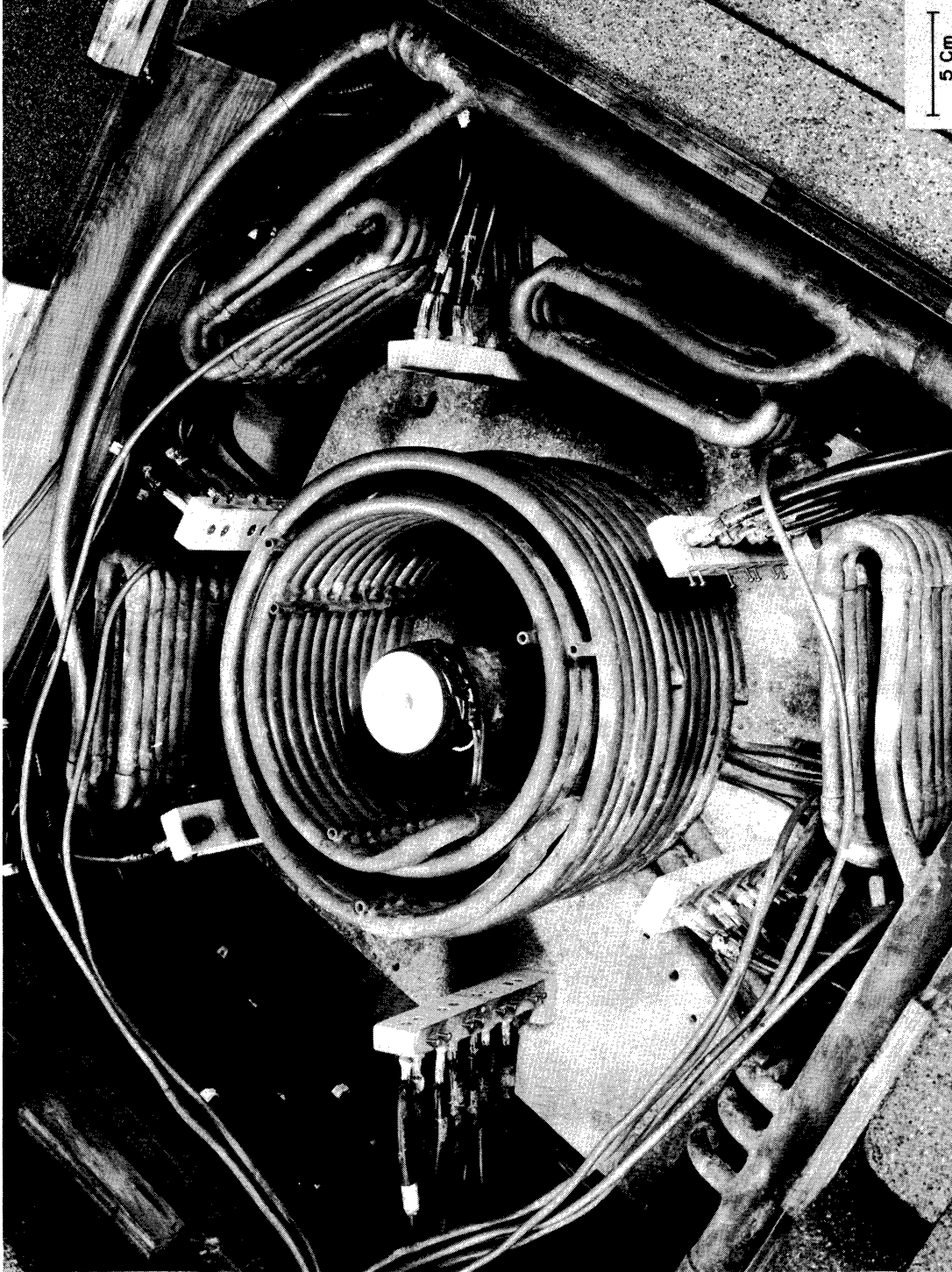


Figure 6. A View of the Zone Melting Apparatus Showing the Heater Supports, Cooling Coils, and Heated Teflon Bearing in the Center.

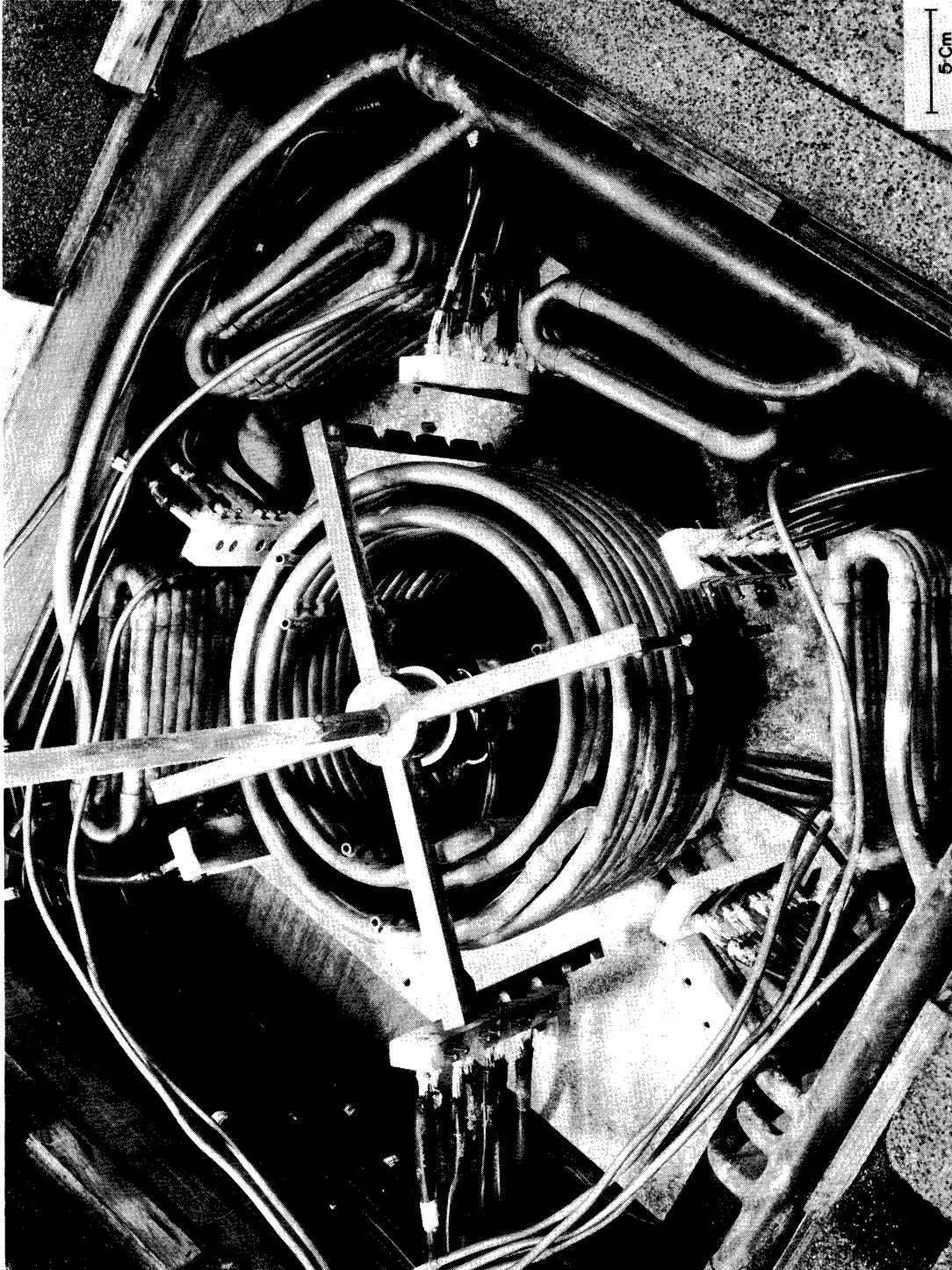


Figure 7. A View of the Zone Melting Apparatus Showing the Merry-go-Round in Position.

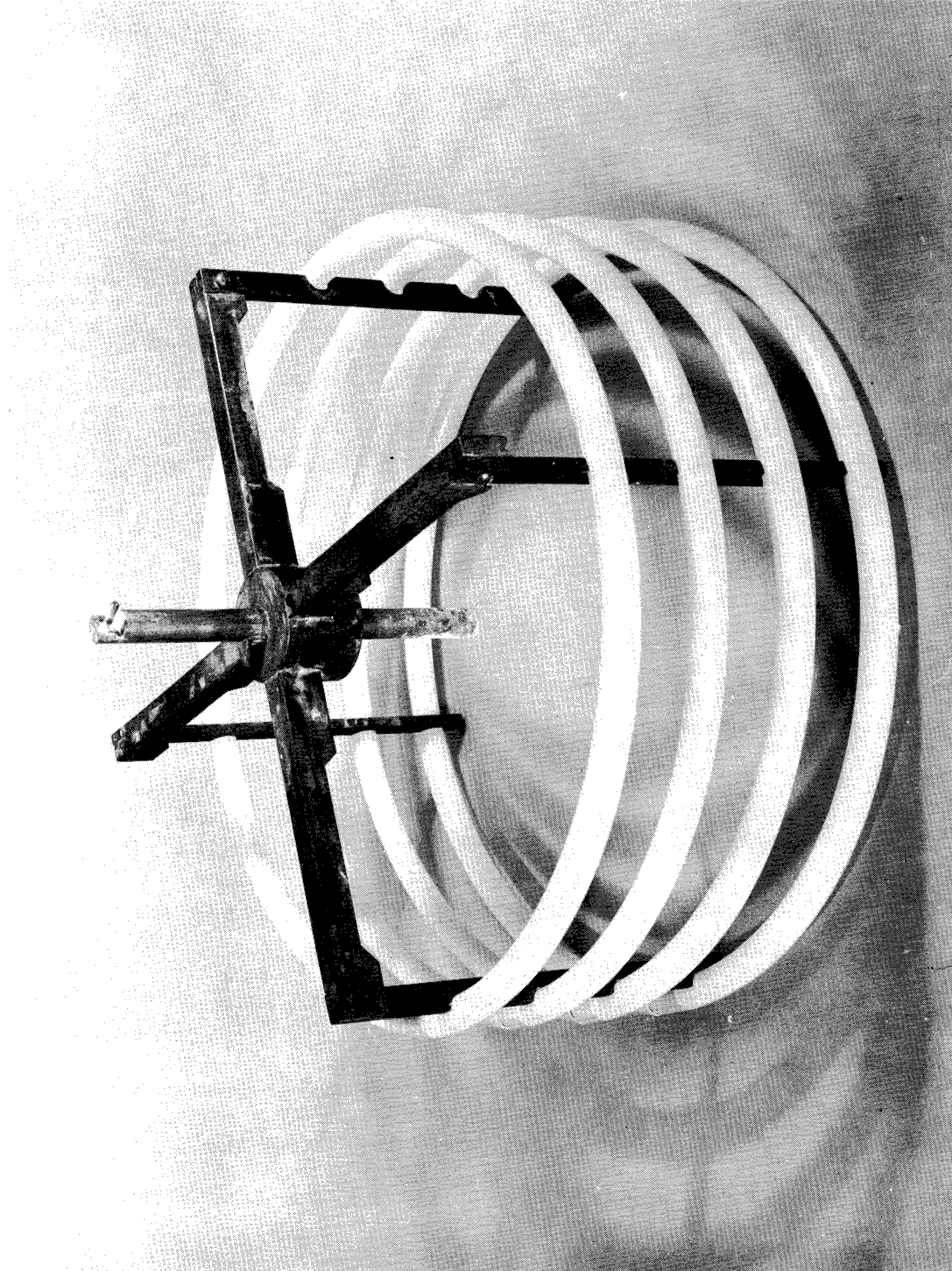


Figure 8. The Sample Tubes on the Merry-go-round.



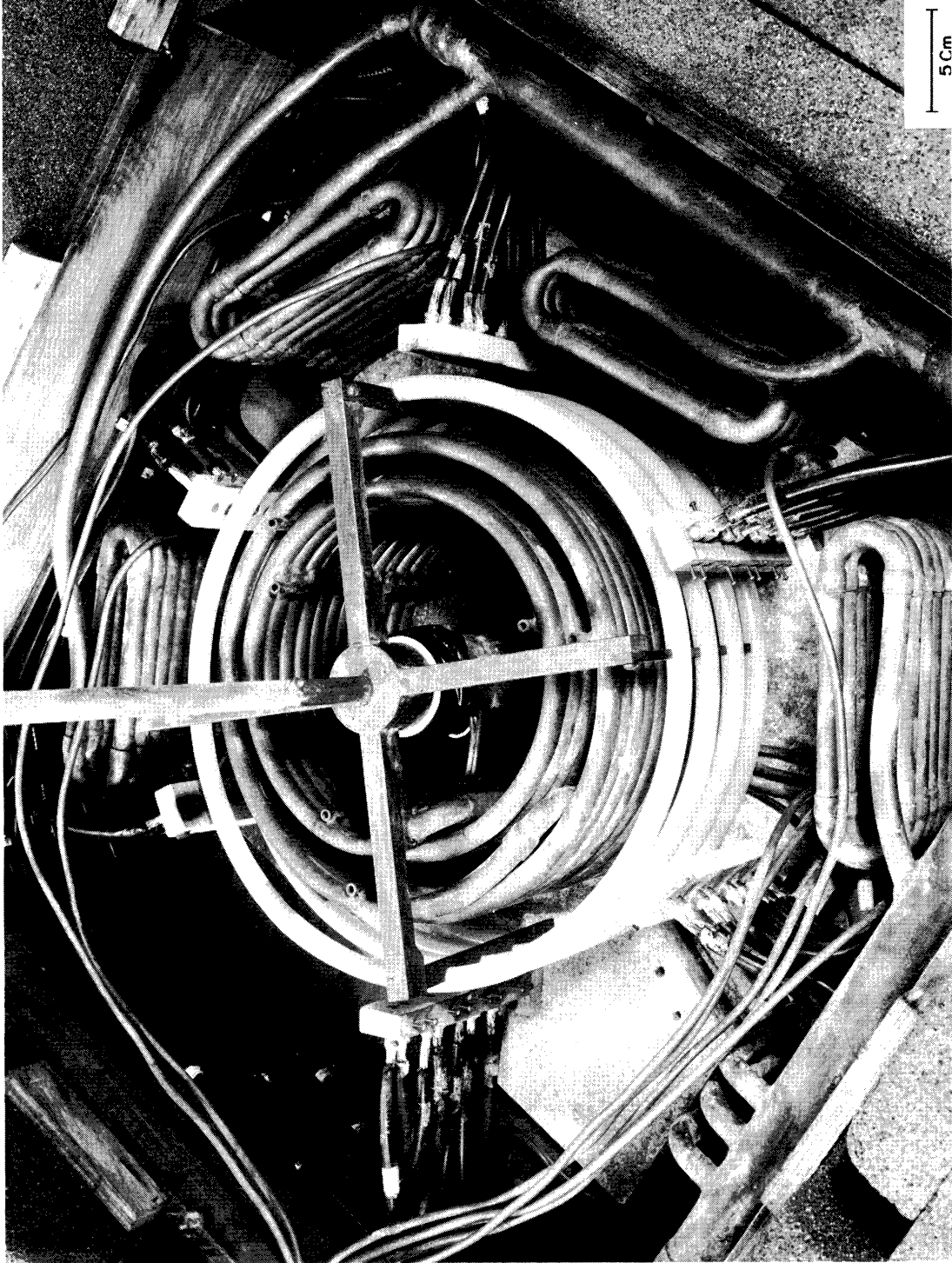


Figure 9. A View of the Zone Melting Apparatus Showing the Sample Tubes in Position.

allowed to melt. Selected sections were examined for the presence of polymer by adding a few drops of the solution maintained above the critical temperature to an excess of methanol, a non-solvent.

Intrinsic viscosities were determined with a Ubbelohde viscometer directly in the cyclohexane used for zone melting in the single phase region at temperatures above any critical temperature. Molecular weight distributions were determined as described above.



## RESULTS AND DISCUSSION

### Static Tests

All static test data on the redistribution of polystyrene between cyclohexane-rich solid and the liquid are plotted as the ratio of the solute's concentration in the solid to its concentration in the liquid vs. the solute's molecular weight. Data are shown both as a function of concentration and of molecular weight distribution in Figure 10 and 11, respectively. In all cases examined, the graphs have an intercept on the ordinate of 1.0 and have a positive slope.

Both increases in concentration and in the proportion of high molecular weight material shift the solid-to-liquid concentration ratio for any species to lower values. On the basis of this evidence, of the three possibilities that can occur on freezing a cyclohexane-rich polystyrene-cyclohexane system - the achievement of thermodynamic equilibrium, non-equilibrium entrapment of a polymer-rich phase in the solid, or non-equilibrium pushing of a polymer-rich phase into the liquid - the possibility of entrapment playing an increasingly important role with an increase in entrapment opportunity is eliminated. It can be noted parenthetically that the occurrence of the inverse trend would indicate that the possibility of the retention of a polymer-rich phase in the liquid could be discounted.

Cooling curve studies were made to determine the relation of the invariant temperatures of polystyrene-cyclohexane solutions to the melting point of cyclohexane. Because a broadly distributed polymer

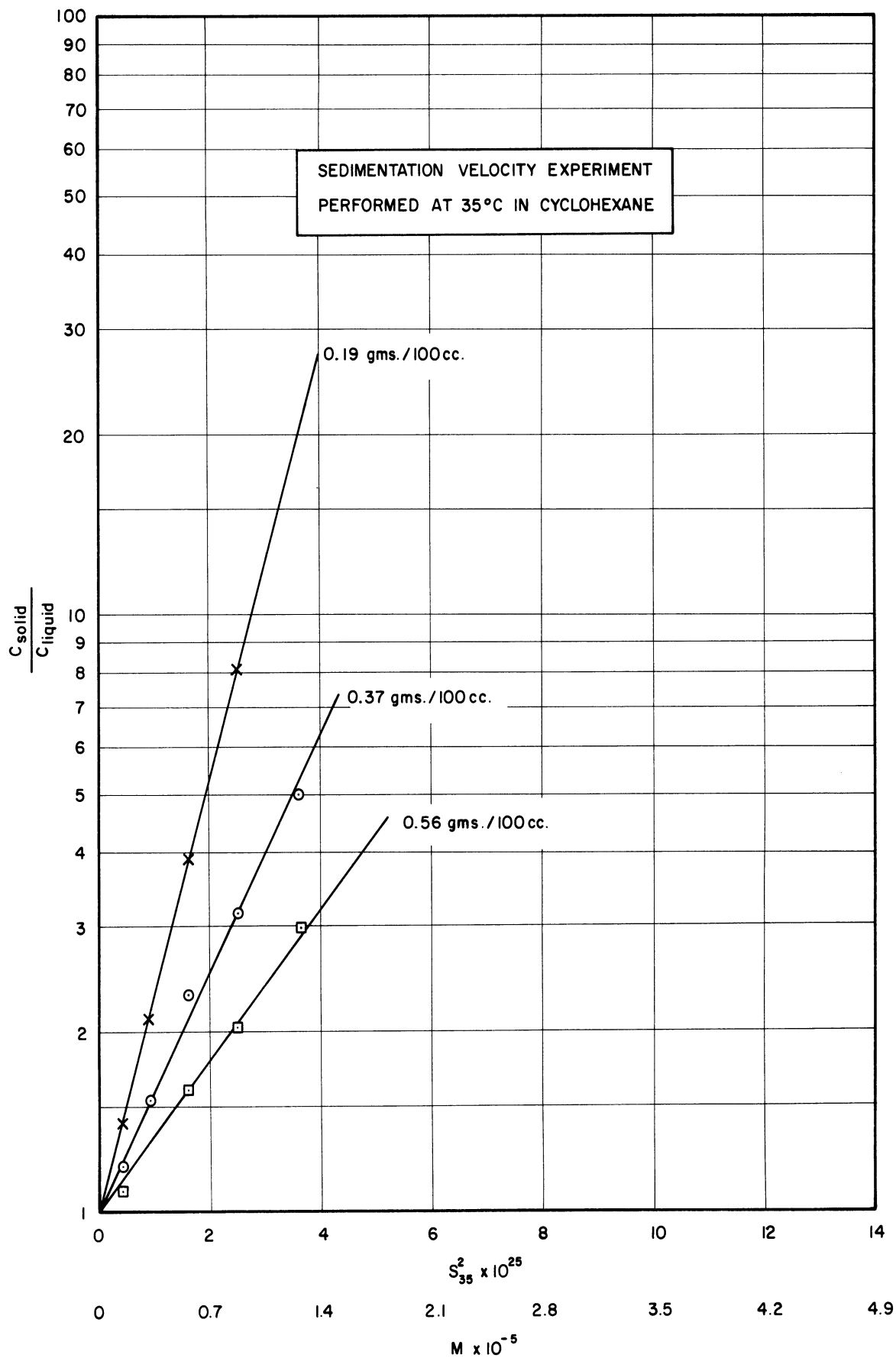


Figure 10. Ratio of Solute Concentrations in the Solid and Liquid vs. Molecular Weight, Determined by Static Tests on Amorphous Broadly Distributed Polystyrene in Cyclohexane.

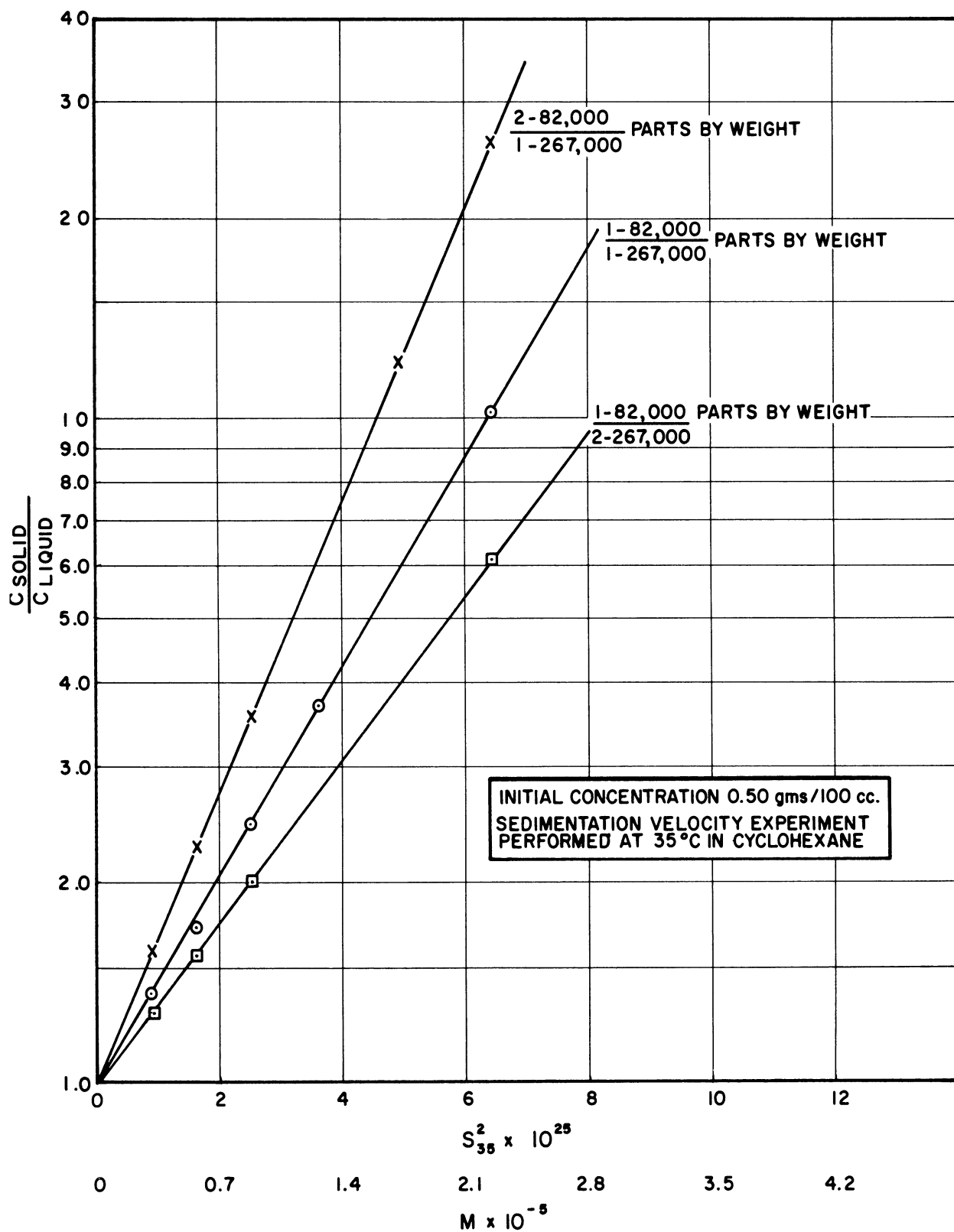
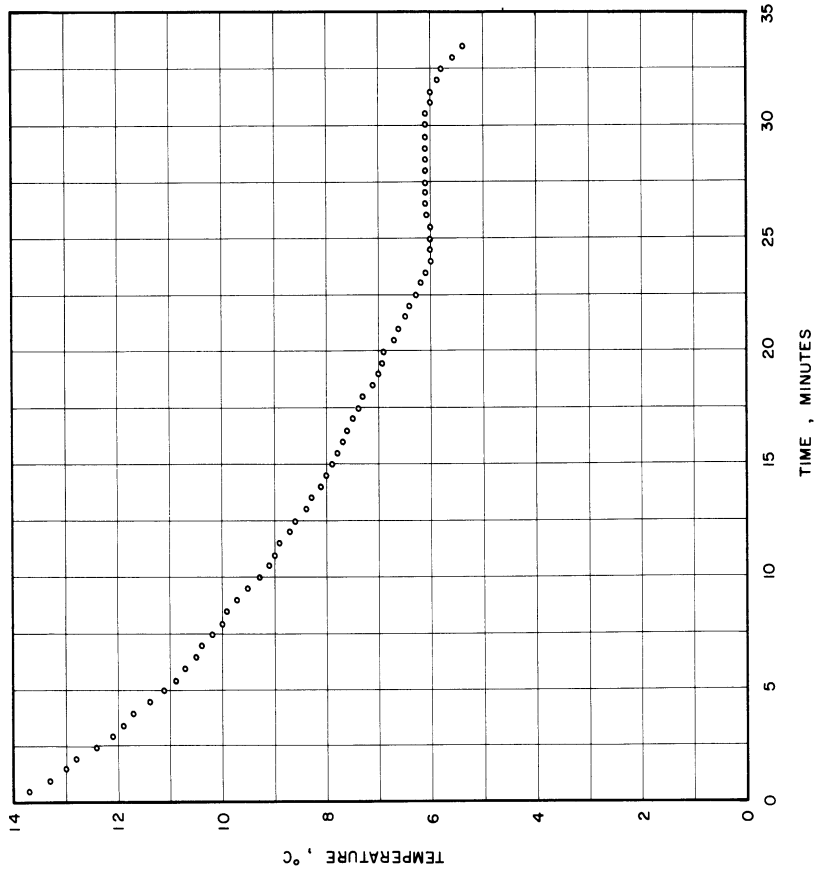


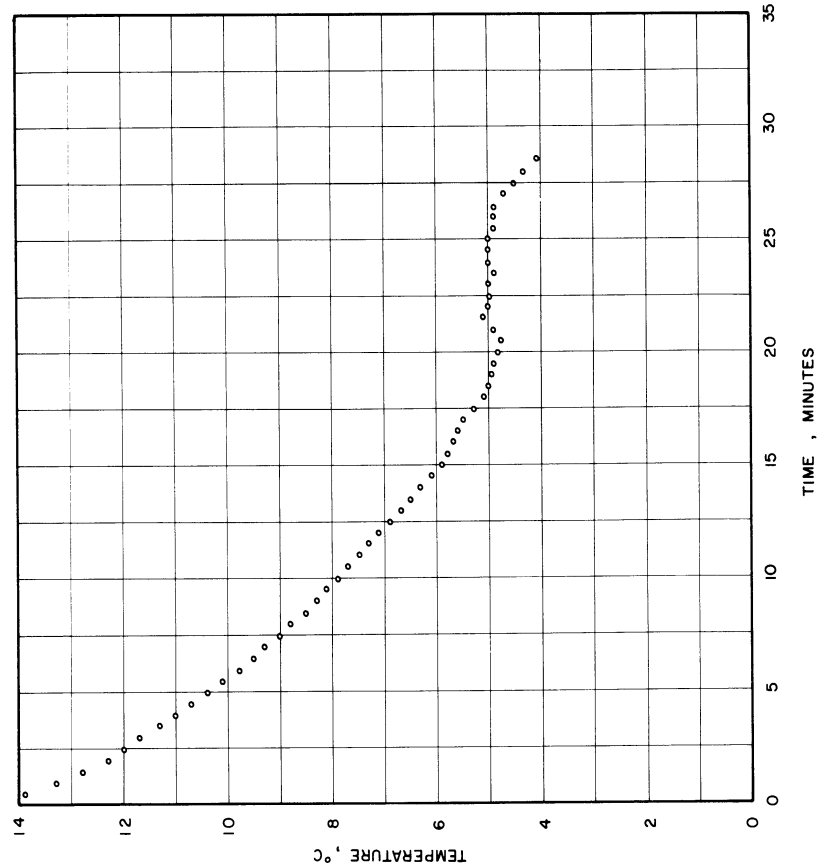
Figure 11. Ratio of Solute Concentrations in the Solid and Liquid vs. Molecular Weight, Determined by Static Tests on Mixtures of Two Amorphous Narrowly Distributed Polystyrenes (MW=82,000 and 267,000) in Cyclohexane.

will display a continuous and difficulty distinguished set of isothermal reactions, the best defined data have been obtained for a system with a narrowly distributed polystyrene in cyclohexane. For example, using the material with a molecular weight of 267,000, Figure 12, an isothermal reaction is clearly indicated at a temperature approximately one full degree above the melting point of the pure solvent. As mentioned in the preceding chapter, the reproducibility of this experiment is sufficiently good to indicate that this difference in temperatures is clearly real. Consideration of binary phase diagrams, wherein the solute either raises or lowers the solvent melting point by means of the existence of an isothermal reaction (Figure 3), shows immediately that the presence of a reaction temperature above the pure solvent melting point gives a ratio of solute concentration in the solid to that in the liquid greater than 1.0.

The very qualitative examination of the extent of attraction of solid solvent for the polymer-rich phase that exists in the liquid region showed virtually no attraction. Advance of the solid toward the polymer-rich phase resulted only in pushing everything in its path ahead of it; retreat left the polymer behind, motionless. Side-to-side motion of the solid past the polymer-rich phase resulted only in minor motion of it as it was moved by the liquid itself that was dragged by the solid. In no case could the incorporation of a particle of the polymer-rich phase into the solid phase be observed even though the experiment was carried out as more solid was being frozen. This evidence confirms the conclusion given above regarding the unimportance of entrapment in freezing this system.



(a)



(b)

Figure 12. Cooling Curves for Cyclohexane-Rich Polystyrene-Cyclohexane Systems: (a) Pure Cyclohexane (b) Cyclohexane With Polystyrene (mw = 297,000); concentration = 1.8 gms./100 cc.

As shown above, static redistribution data provides one conclusion about the occurrence of phenomena on freezing the polystyrene-cyclohexane system. It alone does not permit a distinction to be made between (1) a shift in the thermodynamic equilibrium with changes in total polymer concentration or polymer molecular weight distribution, and (2) an increase in non-equilibrium retention of polymer in the examining the results of the zone melting operation, which will be discussed next.

### Zone Melting Experiments

The results of the zone melting experiments can be conveniently discussed in two categories, (1) the effects of the number of zone passed and of the zone length, and (2) the effects of total polymer concentration and of zone travel rate.

#### The Effects of the Number of Zones Passed and of Zone Length

A sample of the system amorphous polystyrene-cyclohexane was examined over the fraction of its length not subject to the effect of normal freezing in order to determine the locations where changes in the concentrations of species present were most significant for 5 and 6 zones passed (this variable being arbitrarily chosen). As shown by the data in Appendix G, the value of the sedimentation coefficient corresponding to the maximum value of apparent distribution function for each segment changed more in the cases of 1.56 and 2.92 zone lengths than in either of the other pairs of successive segments. This situation is interpreted as meaning that a comparison of all species concentrations in these two segments (i.e.  $1.56 \pm 0.20$  and  $2.92 \pm 0.20$  zone lengths from the head end) would show the best sensitivity to operating variables and they were selected for further study. The breadth of the range of variables, e.g. the number of passes and the spacing of the sample positions, was

intentionally kept small in order to avoid large differences in total concentration of polymer due to excessive redistribution over the ingot's length.

Representative molecular weight distribution curves for a zone travel rate of 4.83 cm. per hour are shown in Figure 13. Detailed data taken from a series of similar curves for experiments with various zone lengths and numbers of zones passed are presented in Table I. An increase in the number of passes or in the zone length results in increasing the difference between the weight-average molecular weight averages. Also noted is a trend for the ratio of breadths at 1/2 peak heights to decrease with increasing number of passes.

The Effects of Total Polymer Concentration and Zone Travel Rate

Zone melting of a mixture of two narrowly distributed amorphous polystyrenes of molecular weight averages of 82,000 and 267,000 dissolved in cyclohexane at a zone travel rate of 4.83 cm. per hour produced an accumulation of the low molecular weight species at the head end of the ingot, whereas the high molecular weight species were localized at the tail end, as indicated by intrinsic viscosity data shown in Figure 14. The lower molecular weight species prefer to remain in the solid under these zone melting conditions, but the higher molecular weight species are carried preferentially in the liquid. A comparison of this result with the theoretical expressions for phase partitioning, (8)

$$\ln\left(\frac{v_i'}{v_i}\right) = x_i \left\{ \left(1 - \frac{1}{x_n}\right) v_2 - \left(1 - \frac{1}{x_n'}\right) v_2' + \chi_1 [(1 - v_2)^2 - (1 - v_2')^2] \right\}$$

shows an inconsistency for the coefficient of  $x_i$  should not change algebraic sign because the two polystyrenes are members of the same structurally homologous series. Further discussion of this observation will be deferred until the remainder of the experimental observations are presented.

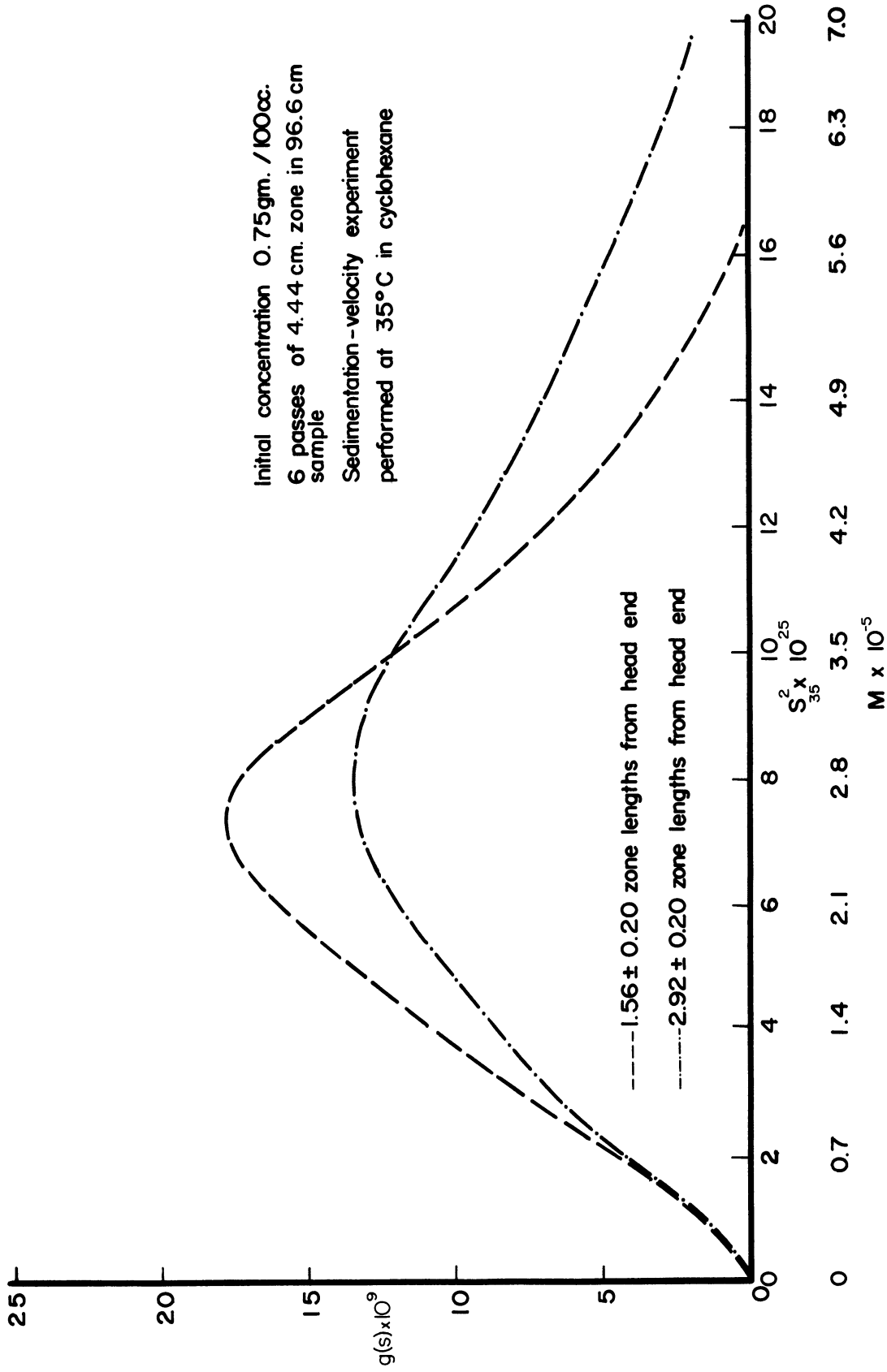


Figure 13. Molecular Weight Distribution Curves of Segments from a Sample of Amorphous Broadly Distributed Polystyrene (PII-58-2-40B) in Cyclohexane Zone Melted at 4.83 cm/hour.



TABLE I

## AMORPHOUS POLYSTYRENE ZONE MELTED IN CYCLOHEXANE

Sample*	Initial Conc. Gm./100 cc.	Final Conc. Gm./100 cc.	Zone Travel Rate Equals 4.83 cm./hour		M <sub>v</sub> (± 5%)	M <sub>w5</sub> -M <sub>v3</sub>	Breadth @ $\frac{1}{2}$ Peak Height	$\frac{(\text{Breadth at } \frac{1}{2} \text{ PH})_3}{(\text{Breadth at } \frac{1}{2} \text{ PH})_5}$
			No. of Zones Passed	Zone Length cm.				
V <sub>2-3</sub>	0.75	0.97	5	4.44	225,000	24,000	315,000	0.74
V <sub>2-5</sub>	0.75	0.86	5	4.44	249,000		424,000	
T <sub>4-3</sub>	0.75	1.16	6	4.44	244,000	32,000	273,000	0.72
T <sub>4-5</sub>	0.75	1.13	6	4.44	276,000		382,000	
V <sub>1-3</sub>	0.75	1.14	5	6.35	181,000	34,000	203,000	0.71
V <sub>1-5</sub>	0.75	1.11	5	6.35	215,000		287,000	
T <sub>3-3</sub>	0.75	1.00	6	6.35	268,000	58,000	294,000	0.67
T <sub>3-5</sub>	0.75	.96	6	6.35	326,000		441,000	
U <sub>2-3</sub>	0.18	0.21	5	4.44	218,000	25,000	210,000	0.74
U <sub>2-5</sub>	0.18	0.21	5	4.44	243,000		277,000	
U <sub>1-3</sub>	0.18	0.22	5	6.35	287,000	32,000	221,000	0.64
U <sub>1-5</sub>	0.18	0.22	5	6.35	319,000		343,000	
U <sub>3-3</sub>	0.18	0.23	6	6.35	201,000	-----	238,000	---
U <sub>3-5</sub>	0.18	0.19	6	6.35	-----	-----	-----	---

\* Samples labeled "-3" refer to segments taken 1.56 ± 0.20 zone lengths from the head end; samples labeled "-5" refer to segments taken 2.92 ± 0.20 zone lengths from the head end.

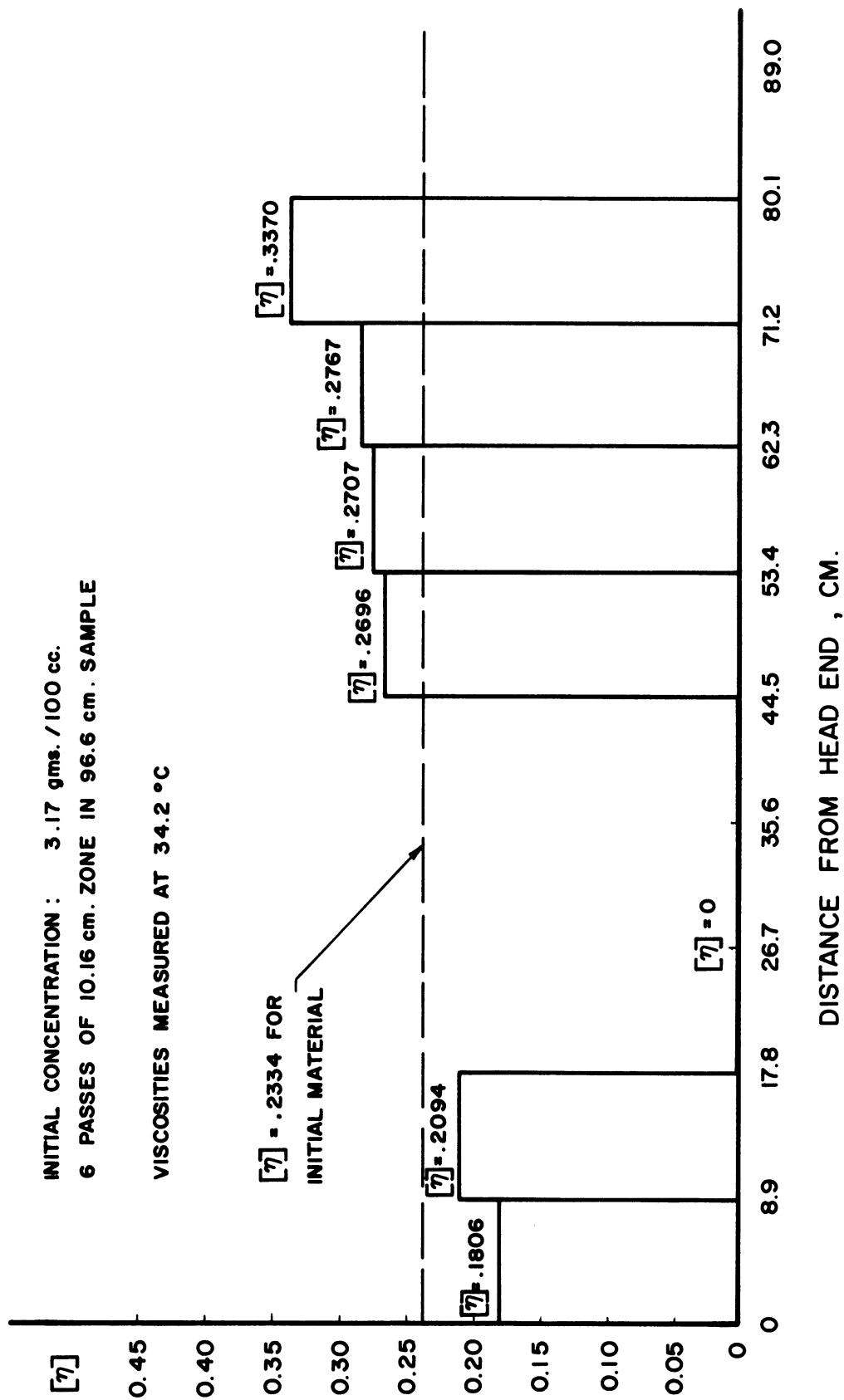


Figure 14. Intrinsic Viscosity vs. Sample Position After Zone Melting a Mixture of Two Amorphous Narrowly Distributed Polystyrenes (MW = 82,000 and 267,000) in Cyclohexane at 4.83 cm/hour.

In order to verify the results of the experiment using two different narrowly distributed materials, attention was directed toward the broadly distributed amorphous polystyrene. It is apparent for this situation that average values as indicators of the redistribution effects would not be as informative as molecular weight distribution data. However, in order to discern any regularly occurring phenomena from the sheer volume of data obtained, a systematic, economical method of data analysis is needed. For this purpose, the raw data are "reduced" by determining ratios for various species (i.e. molecular weights) at two selected locations of the ingots as a function of the operating variables. Thus, any change in solute behavior is directly noticeable upon examining the ratios alone. An additional advantage of this approach is the fact that in the event that thermodynamic partitioning is indeed being approached, effective segregation coefficients can be obtained via Lord's solution<sup>(15)</sup> and these can be extrapolated via Burton's approach<sup>(3)</sup> to obtain equilibrium segregation coefficients for the various species. The sample locations described in the previous section were also employed here.

Graphs of concentration ratios vs. molecular weight are given in Figures 15, 16, 17, and 18 for ingots of various number of zones passed, initial concentrations, and rate of advance of the zones. It can be readily seen that for rates of zone travel 4.83 cm./hour or greater, the curves begin at 1.0, go through maxima at ratios greater than 1.0, and then decrease sufficiently to go below 1.0. The species with ratios greater than one prefer the solid, while those with ratios less than one demonstrate a preference for the liquid. The direction

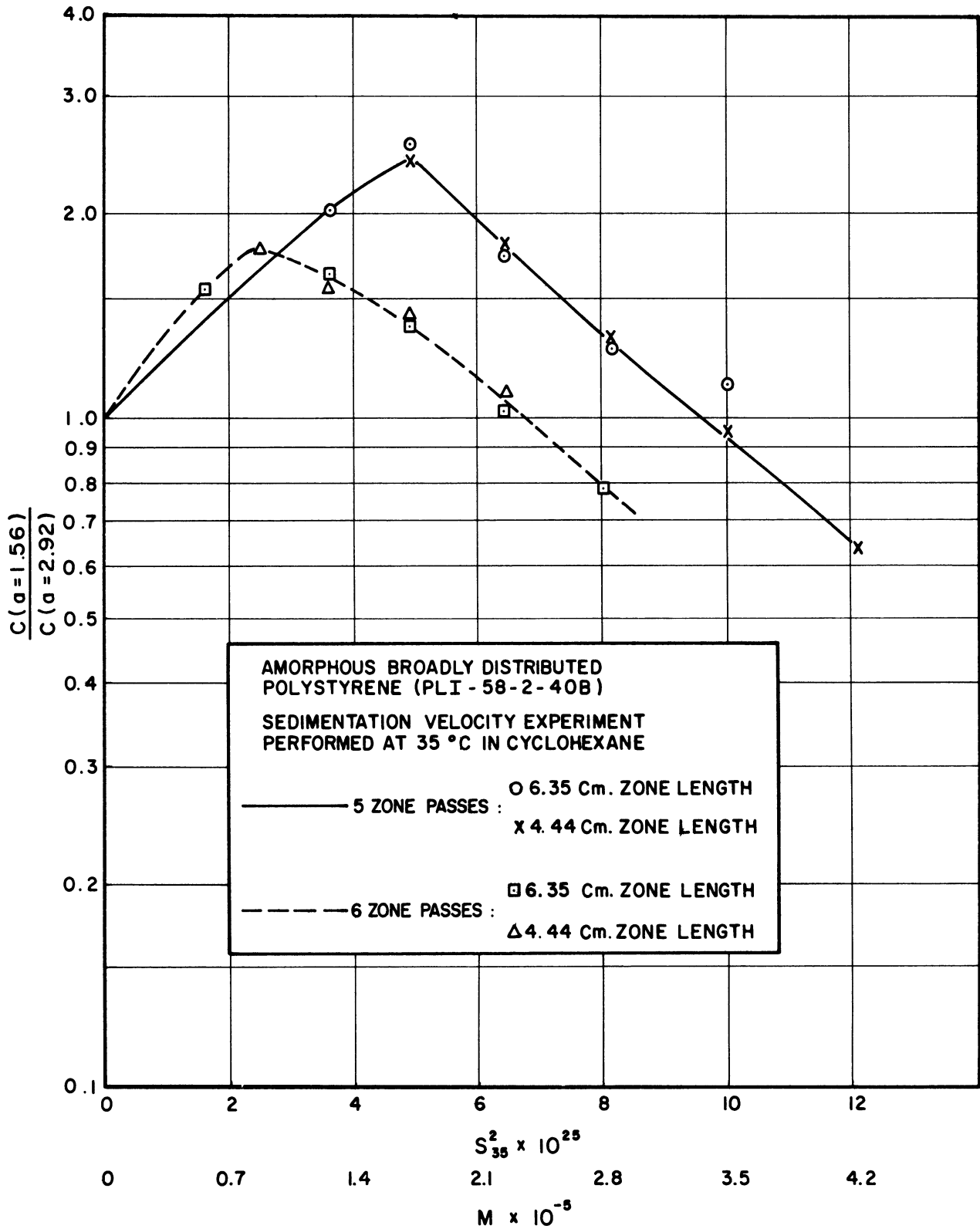


Figure 15. Ratio of Solute Concentrations at 1.56 and 2.92 Zone Lengths from the Head End vs. Molecular Weight, Resulting from Zone Melting 96.6 cm. Samples at 4.83 cm/hour: Concentration 0.18 gm/100 cc.

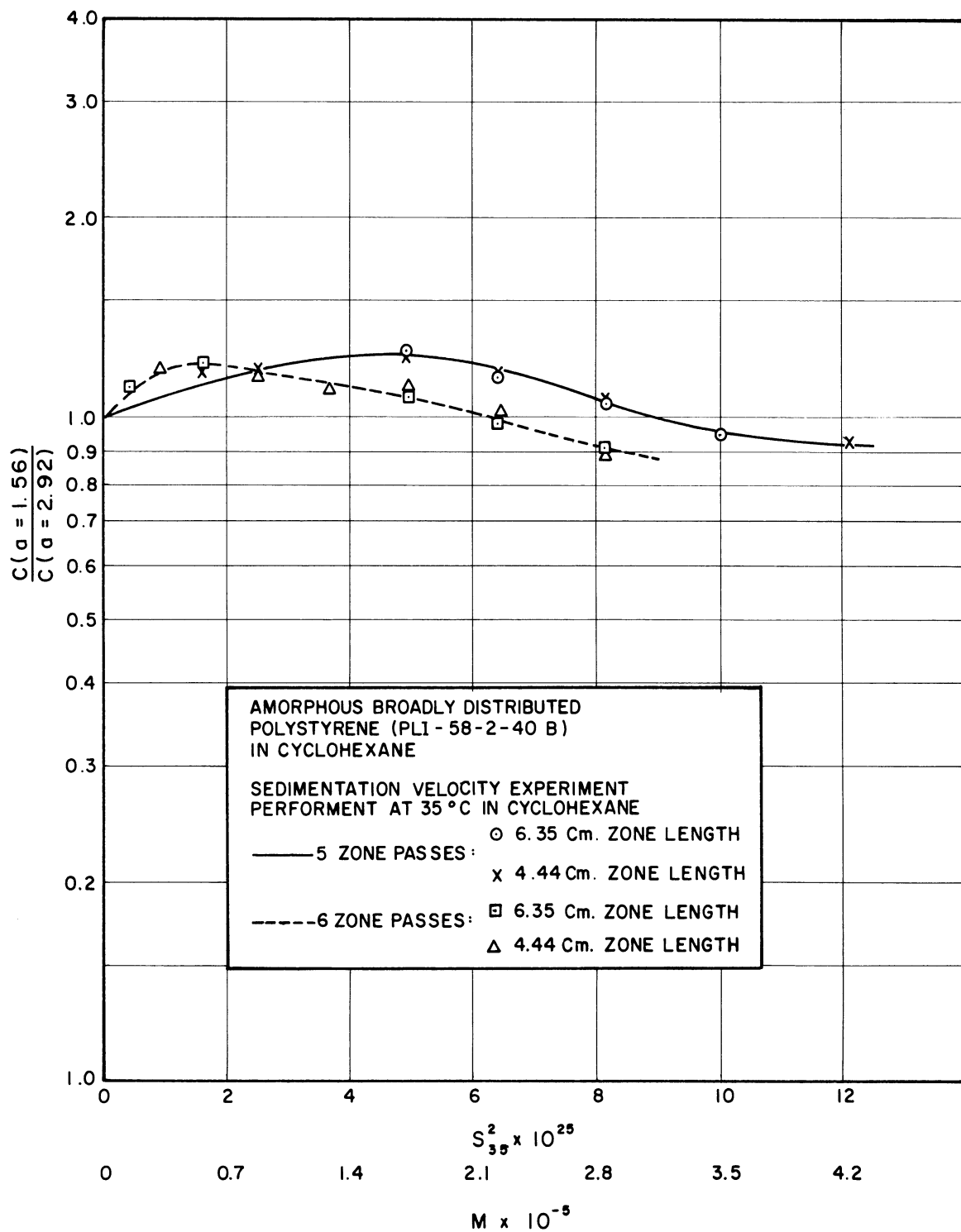


Figure 16. Ratio of Solute Concentrations at 1.56 and 2.92 Zone Lengths from the Head End vs. Molecular Weight, Resulting from Zone Melting 96.6 cm. Samples at 4.83 cm/hour: Concentration 0.75 gm/100 cc.

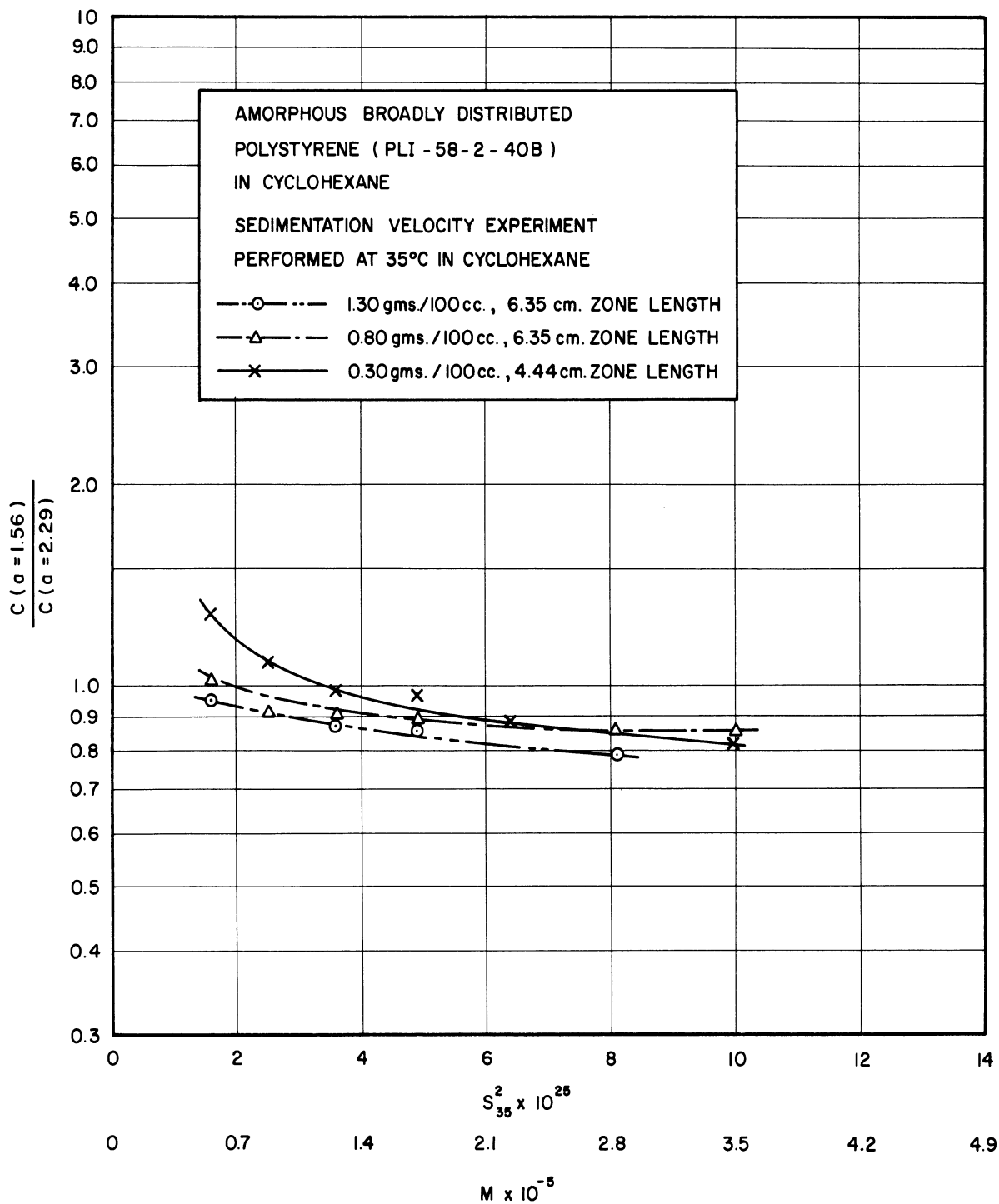


Figure 17. Ratio of Solute Concentrations at 1.56 and 2.92 Zone Lengths from the Head End vs. Molecular Weight, Resulting from Zone Melting 96.6 cm Samples at 9.66 cm/hour: 5 Zones Passes.

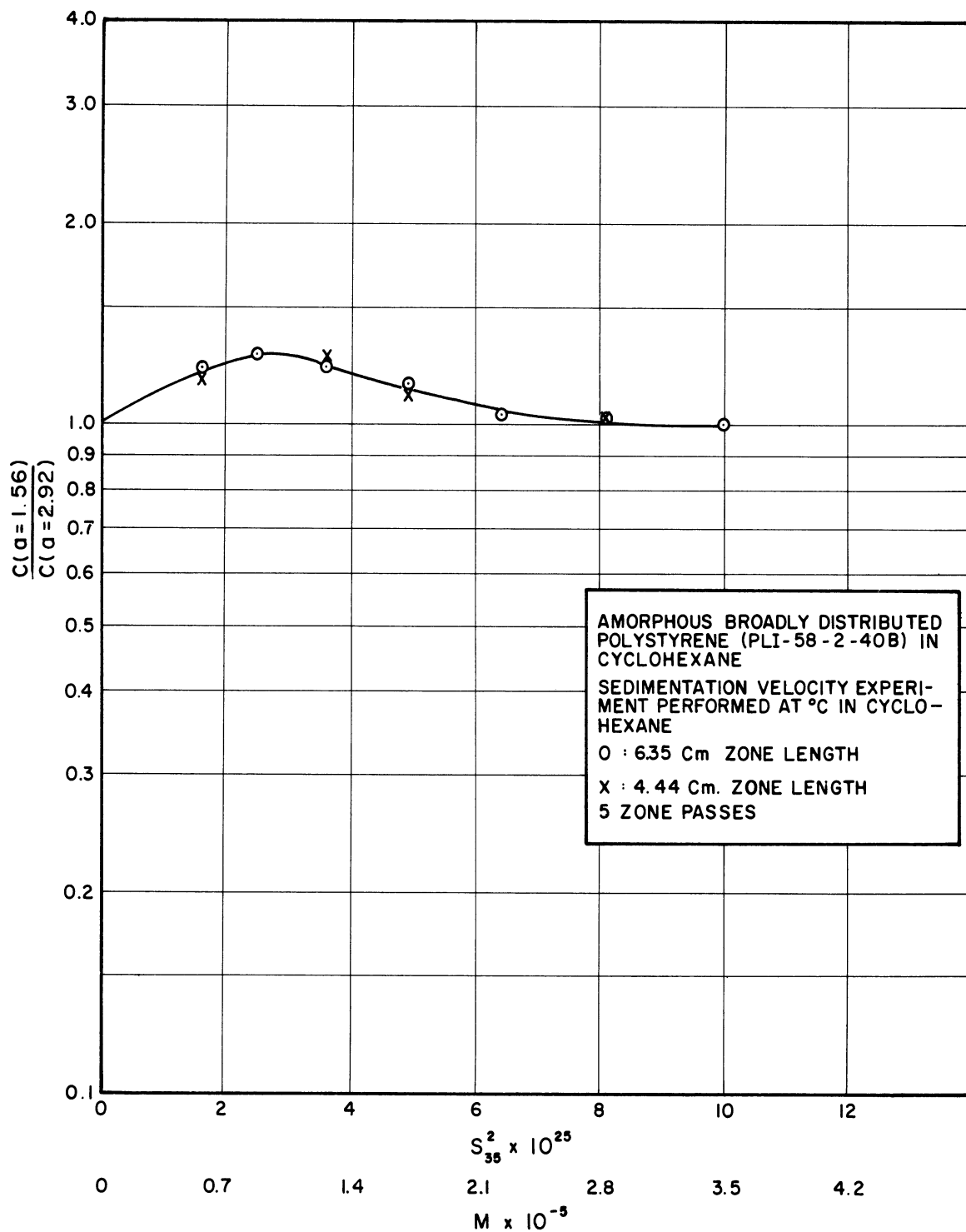


Figure 18. Ratio of Solute Concentrations at 1.56 and 2.92 Zone Lengths from the Head End vs. Molecular Weight, Resulting from Zone Melting 96.6 cm, Samples at 4.01 cm/hour; Concentration 0.75 gm/100 cc.

of this variation, i.e., with smaller molecules having their ratios greater than one and the larger molecules have their ratios less than one, confirms the results found simply by examining the intrinsic viscosity-position relationship for the zone melted ingot with two narrowly distributed polystyrenes.

The slopes of the curves increase with the number of zones passed, indicating increased redistribution, as is to be expected. This results in crossover from greater than one to less than one to occur at lower molecular weights with increased extent of zone melting.

An increase in the initial concentration results also in a shift of the concentration ratio for the various species. The species with concentration ratios greater than one are reduced with increased concentration, and those with ratios less than one are increased with increased concentration when the zone travel rate is 4.83 cm./hour. The net result is a reduction of the gradient with increased concentration. The fact that in the case where the zone travel rate is 4.83 cm./hour, the point of crossover through 1.0 is the same for both concentrations (for a given number of zones passed) is coincidental; there seems to be no correlation of this point in the case where the zone travel rate is 9.66 cm./hour.

In the case where the rate of zone travel is reduced to 4.01 cm./hour, the concentration ratio at no time is less than 1.0. Because the slower rates should more nearly approximate the thermodynamically controlled situation, these data were compared with those that would obtain as calculated from Lord's equation (see Appendices C and D). The ratio of  $C_n(a)$  to  $C_0$  was computed for various combinations of the variables  $k$ ,  $n$ , and  $a$  (the effective segregation coefficient, the number of zones passed, and the location in the ingot measured in zone lengths from the head end, respectively) according to the program given in Appendix C. Ratios of  $C_n(a = 1.56)$  to  $C_n(a = 2.92)$  were then computed and the results plotted as a function of the segregation coefficients given rise to the ratios, as in Appendix D. Ambiguity in the choice of segregation coefficient for cases where the ratio of concentrations is greater than one is resolved by assuming a monotonic relation for segregation coefficients vs. molecular weight. In this way, effective segregation coefficients could be assigned



to the species, and these results are shown in Figure 19. The linearity of the semilogarithmic plot conforms to the thermodynamic theory.

It will be noted from the graph of the pertinent calculations in Appendix D that for  $K_{\text{eff}}$  greater than 1.0, a given extent of zone melting produces diminishing ratios of solute for two locations not at the head end of the ingot with increasing  $K_{\text{eff}}$ . This is simply the result of the concentration of solutes approaching a constant value at ingot locations remote from the head end. This phenomenon has occurred in the above case, and gives rise to the maximum in the curve.

Three factors mentioned so far - that is, the reverse in slopes for single experiments conducted at the faster rates of zone travel, the drastic change from a positive slope with no concentration ratios less than 1.0 to a negative slope with ratios both greater and smaller than 1.0, and the ability to obtain a semilogarithmic plot for the effective segregation coefficient (in agreement with thermodynamic theory) - suggest that a rate phenomenon is controlling the redistribution of solute species in the faster experiments.

A rate process to be considered at the outset is diffusion of solute species from the bulk liquid to the interface. Burton's analysis, described in the literature survey, shows unequivocally that this process alone cannot shift an effective segregation coefficient to the opposite side of 1.0 from the equilibrium value. Since the data reported above are on both sides of 1.0, this process must be discounted as the main factor giving rise to the unusual redistributions observed.

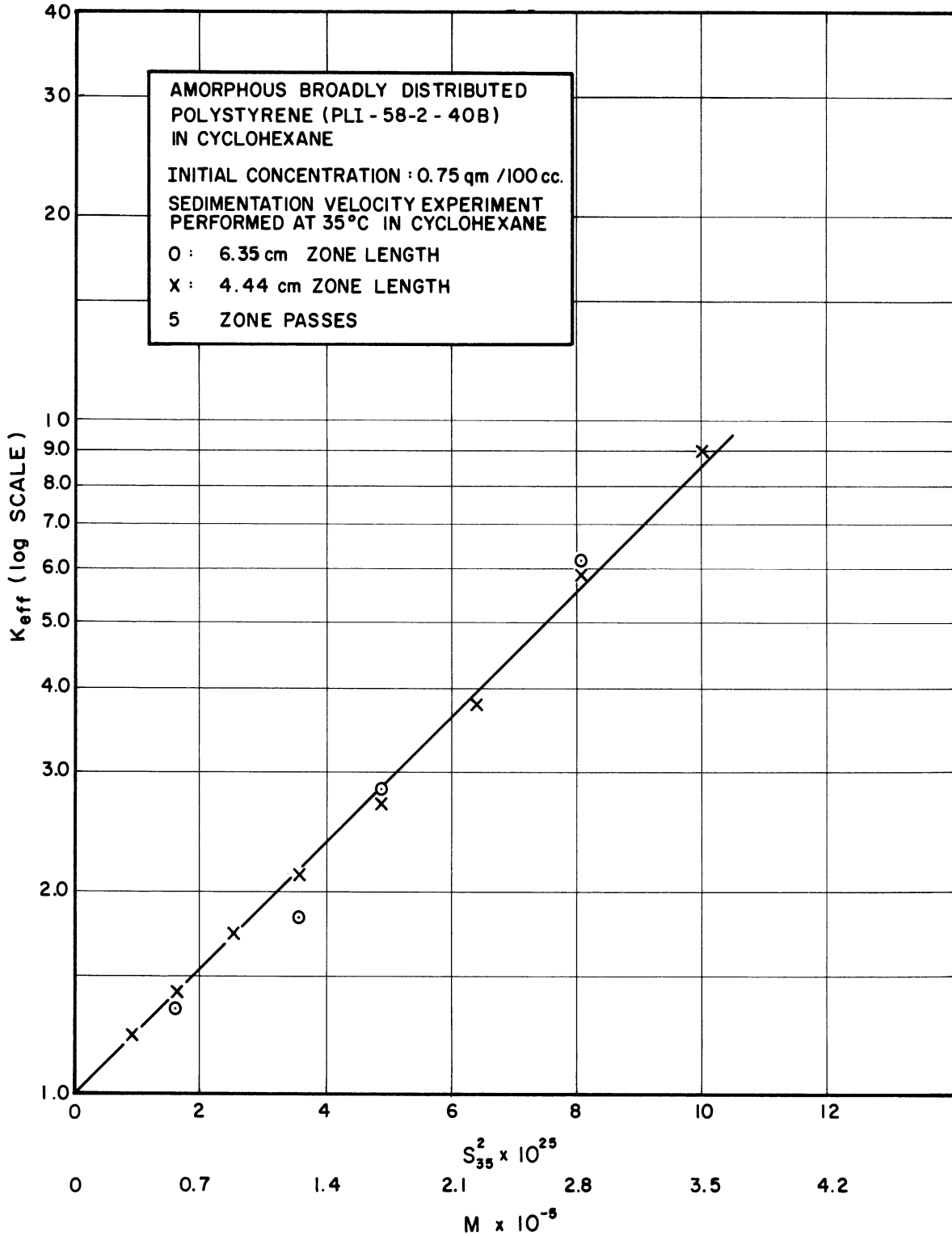


Figure 19. Effective Segregation Coefficient vs. Molecular Weight, Determined by Zone Melting 96.6 cm. Samples at 4.01 cm./hour.

All other rate processes involve the establishment of thermodynamic equilibrium, and can be categorized into two groups. On one hand is entrapment in the solid of solute species which really belong in the liquid. On the other hand is the slowness with which the polymer-rich phase (Y in Figure 3) enters into the three-phase equilibrium reaction (resorption) compared to the rate of advance of the freezing interface.

Entrapment has been discounted in the static tests, and a similar conclusion can be reached on the basis of the effects of zone travel rate and of total concentration in the zone melting experiments themselves. Consequently, the rate-controlling process involves the polymer-rich phase breaking down to provide solute species which are truly more soluble in the solid than in the liquid.

If the time necessary for the three-phase reaction to occur is longer than the time allowed by the advance of the freezing interface, the polymer-rich phase will be pushed along in the liquid. This results in the concentration ratios' being less than 1.0, even though the equilibrium values would be greater than 1.0. Any process which enhances the formation or retention of the second phase in the liquid in the zone melting experiment contributes to an increase in the polymer carried in the liquid toward the tail end of the ingot. Thus, increased total concentration of polymer or increase proportion of high molecular weight components result in more species being carried in the liquid.

For a given initial concentration, each zone pass builds up the concentration toward the head end of those species which are small enough to resorb for that pass in the time available. However, at the same time these species approach the concentration for which resorption

is no longer possible in the time available, and the crossover point through 1.0 decreases with each successive pass.

The decrease in the magnitude of the slope of the curves of concentration ratios vs. molecular weights upon increased total initial concentration or zone travel rate (at rates greater than 4.83 cm. per hour) is attributed to a decrease in mobility of the individual species that comprise the polymer-rich phase under these conditions. At higher concentrations, the opportunities for entanglement are greater and the extent of redistribution for all species is lessened considerably. At the higher rate of zone travel, solidification is so much more rapid than the three-phase reaction that the amount of polymer-rich phase retained in the liquid is appreciably increased, giving the same effect as an increase in total concentration.

Reduction of the amount of polymer-rich phase through the resorption reaction is a diffusion-controlled process, which occurs in the polymer-rich phase itself, not in the liquid boundary adjacent to the advancing freezing interface. A confirmation of the validity of the above explanation of the redistributions observed can be obtained by comparing the diffusion velocity with the rate of zone travel. The mathematics of the comparison are presented in Appendix E. Implicit in the comparison is the assumption that diffusion velocities of polymer species in the cyclohexane-rich liquid and in the polymer-rich phase are of the same order of magnitude. Since both phases are non-crystalline, as a first-order approximation this procedure is deemed reasonable. The results of the calculation show that indeed the diffusion velocity is comparable to the rates of advance of the freezing interface.

Even if the slowness of resorption is acknowledged as a primary factor causing the unusual behavior presented above, it alone does not explain why the behavior, measured in terms of concentration ratios, is intermediate between the thermodynamic situation and the non-equilibrium extreme. It would be expected, at first glance, that for a given molecular weight species the behavior would be either of one kind or the other, but not both, which is necessary to give the intermediate value measured. This apparent difference between expected and observed behaviors can be explained by considering the crystallization and melting of a polymer from a dilute solution.

Till<sup>(30)</sup> has found that there exists a range of abilities of a polymer to crystallize out of dilute solution as function of such features as chain length heterogeneity, chain entanglements, and the presence of side branches. The chains which do not actually form crystallites upon precipitation are then found in a range of orientation perfection (where the highest degree of orientation is the 100% crystalline arrangement). It is a well-known fact that the melting process for such a range of orientation perfection occurs over a small, but not-infinitesimal temperature range. This fact indicates that a system of monodisperse chains in a range of orientation perfection requires a range of increments of activation energy to undergo a change in state. As a result, for any given condition, for a system of monodisperse chains, some of the chains can undergo transition while others cannot. Thus, some of the chains will be resorbed, but not necessarily all of them will be resorbed in any finite time. Consequently, small

variations in the rate of interface advance cause the time available for resorption to shift from a sufficient amount for the majority of any species to an insufficient amount, and causes the unusual behavior reported above to occur.

## CONCLUSIONS

Redistribution of polystyrene in cyclohexane by zone melting dilute solutions (up to 1-1/2 gms. of polymer per 100 cc. of solution) can occur on either of two bases, which are somewhat competitive. The rate of zone travel determines which basis predominates.

At slow rates of zone travel (4.01 cm./hour or less) redistribution of solute species occurs in conformity with thermodynamic predictions. In this case, a cyclohexane-rich liquid and a polymer-rich liquid, which coexist at temperatures just above the solidification range, react to form a cyclohexane-rich solid solution upon solidification. The solid solution contains a higher concentration of all polymer species than does the cyclohexane-rich liquid, with the ratio of the concentration in the solid to the concentration in the liquid increasing exponentially with molecular weight of the solute. The net result is the accumulation of all solute species toward the head (i.e. first melted and first frozen) end of the zone melted ingot, with the higher molecular weight species enjoying the greatest redistribution in this respect.

At moderately faster speeds of zone travel (ca. 4.83 cm./hour) resorption of some of the higher molecular weight species from the polymer-rich phase is not sufficiently fast compared to the rate of freezing, so that some of the polymer-rich phase remains after solidification and is simply carried in the moving liquid zone. The net result is a reversal in the accumulation trend with molecular weight: the higher

molecular weight species are carried increasingly to the tail (i.e. last frozen) end of the ingot. Increases in total polymer concentration enhance this effect.

At significantly faster speeds of zone travel (ca. 9.66 cm./hour) the lack of sufficient opportunity for the resorption reaction to occur is greater. However, the resulting increased polymer concentration in the liquid zone gives rise to lessened mobility of the polymer-rich phase. The net effect in this case is a decreased redistribution of solute species: they are merely incorporated into the advancing solid with little selectivity. Increased total polymer concentration reduces the selectivity.

For an initially broadly distributed polymer, in no case can a single species be localized by zone melting a dilutely concentrated ingot without the presence of considerable quantities of slightly smaller and slightly larger molecules. However, proper choice of the total polymer concentration and rate of zone travel can allow rough separations to be effected; suitable combinations of successive zone melting operations may permit a moderate degree of fractionation to be achieved.



## APPENDIX A

### ZONE MELTING APPARATUS

The zone melting apparatus consists essentially of 4 parts: the shell, the electrical heating system, the refrigeration system, and the motive system.

#### The Shell

The shell consists of two square boxes of 1-1/2 cm. plywood, one inside the other, separated by 9 cm. of foam glass insulation. A split top consisting of 9 cm. of the same insulation supported on plywood is positioned inside the wall created by the inter-box insulation and is supported on the edges of the inner box. The inside dimensions of the box are approximately 62 cm. x 62 cm. x 20 1/2 cm. deep. A small semicircular hole cut in the center of the "split face" of each section of the top allows the drive shaft to extend outside the box. The shell is shown in Figure 6.

In the event of very warm and/or humid weather, the insulating qualities of the shell are enhanced by covering it with polyethylene film in order to reduce the influx of warm and/or moisture-laden air through the split and other joints on the top. Particularly to combat the formation of frost, a dessicant, such as  $\text{CaCl}_2$  or Drierite, is placed in cheesecloth bags under the polyethylene. Occasionally, it has been found necessary to treat the wood parts of the shell near joints with an antifogging agent in order to reduce the accumulation of frost or ice at these points.

### The Electrical Heating System

Radiant heating is provided locally by 20 gauge Chromel A resistance heating wires 1-1/4 cm. long between parallel brass connectors. The brass connectors are held in a transite column mounted on an aluminum base which covers most of the floor of the shell. Electrical power is provided to each wire from the secondary of 30 to 1 voltage transformers at a maximum voltage and current of 4 volts and 50 amperes, respectively. The low voltage is used to prevent arcing through the air from one circuit to another closeby. Power is fed to the voltage transformers from auto-transformers connected to a 110 volt line. Both voltmeters and ammeters, as well as glow lamps, are installed in the circuits to monitor their operation. The heating posts can be seen in the photograph of the inside of the dismantled apparatus (Figure 6).

### The Refrigeration System

Refrigeration is provided by evaporating Freon 22 in copper coils, which can be seen in Figure 6. The coils are placed to provide the greatest possible heat sink to the samples as they move away from the heaters, as well as to maintain the ambient temperature below the melting point of the system. The refrigerant is compressed by a 5 horsepower unit equipped with a water-cooled condensor. The net capacity of the cooling system under service conditions is approximately 2400 watts at -40°C.

### The Motive System

Samples in the shape of toroids are carried horizontally on a merry-go-round which is supported on a heated Teflon bearing at the

center of the apparatus and which is driven by a shaft passing through the top of the box to a small motor positioned above. The merry-go-round is shown in position in Figure 7.

## APPENDIX B

### THE FABRICATION AND FILLING OF SAMPLE TUBES

Samples of the polystyrene-cyclohexane solutions were contained in Teflon tubing in the shape of toroids. This material was selected rather than glass because of its relative ease of forming and because it can withstand stresses induced by the severe volume changes that accompany phase changes in organics.<sup>(23)</sup>

The toroids are formed from straight lengths of tubing  $1.161 \pm 0.025$  cm. I.D. and  $0.051 \pm 0.013$  cm. thick by slipping them onto an internally steam-heated, chrome-plated steel ring, which is shown in Figure 20. Chrome plating was found necessary to reduce the friction and to reduce the transfer of rust to the Teflon. After the circular shape has been formed, cold water is substituted for the steam, and the ring and the Teflon are cooled. The cold Teflon is then unwound from the ring.

The Teflon is cut to the proper length (96.6 cm. median circumference). The ends are treated momentarily with a one-normal solution of sodium naphthalene in tetrahydrofuran<sup>(20)</sup> to make the material amenable to using an adhesive.

Brass rod is machined to the inside diameter of the tubing and bent to the curvature of the desired toroids. Segments are cut from the rod to serve both as plugs and as fasteners of the two ends of the toroids.

One end of a brass plug is fastened to one end of a toroid with epoxy resin and allowed to set. Upon the setting of the resin, the

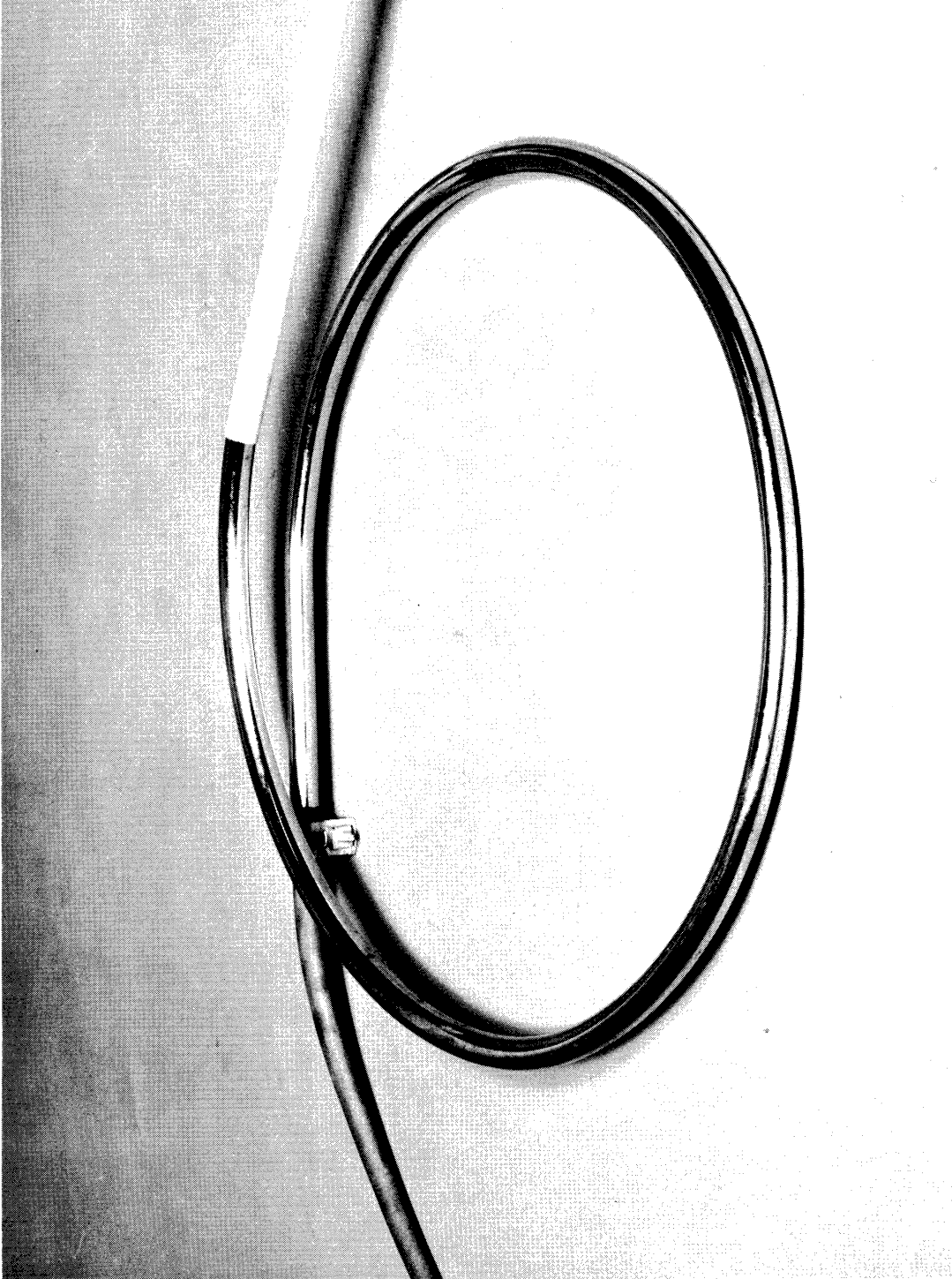


Figure 20. Steam-heated, Chrome-plated Steel Ring for Forming Teflon Torroids.

toroid is filled with the desired solution, the other end of the plug is slipped simply into place, and the filled assembly is placed horizontally in a freezer to solidify. After solidification has been completed, the loose end of the brass plug is removed from the Teflon tube and reinserted with an application of epoxy resin to fasten it in place. This operation is performed while the solution is still maintained in the solid state by having the toroid mounted on a pre-chilled aluminum plate, as shown in Figure 21. The completely assembled tube still mounted on the aluminum plate is then returned to the freezer to await the setting of the final joint.

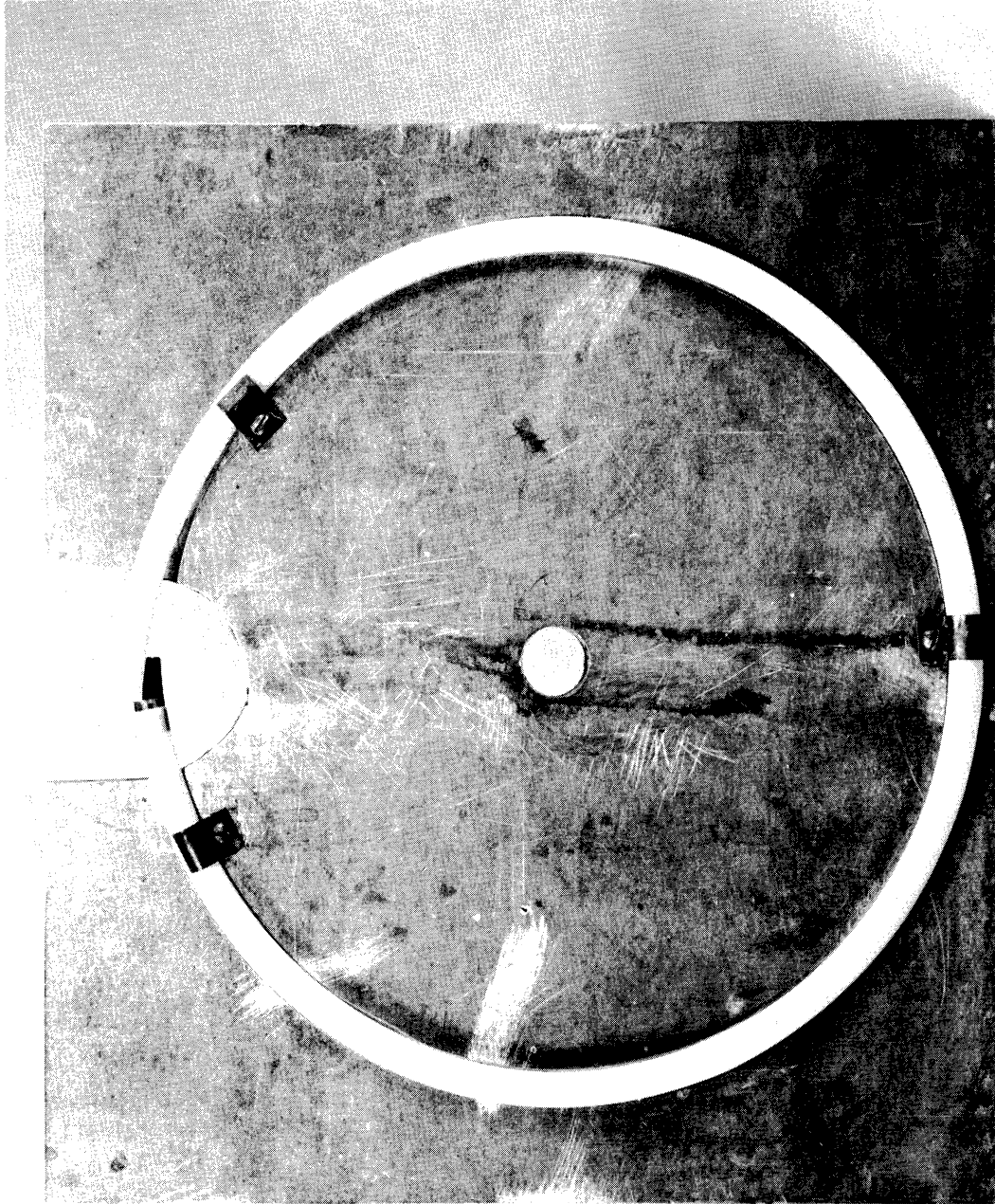


Figure 21. Aluminum Plate Used to Maintain Samples Chilled During Their Preparation.

APPENDIX C

COMPUTER PROGRAM FOR THE SOLUTION OF LORD'S EQUATION<sup>(15)</sup>  
 FOR THE ZONE MELTED SEMI-INFINITE INGOT IN BENDIX ALGORITHM  
 DECODER LANGUAGE FOR USE ON A BENDIX G-15 COMPUTER

$$\frac{C_n(a)}{C_0} = 1 - [(1-K)e^{-Ka}] \left[ n - \sum_{t=1}^{n-1} \sum_{s=1}^t e^{-sK} K^{s-1} \sum_{r=0}^{s-1} \frac{s^{s-r-2} a^r (r+1-Ka)}{(s-r-1)! r!} \right]$$

where C is the solute concentration  
 K is the effective segregation coefficient  
 n is the number of zones passed  
 a is the distance in the ingot from the head end measured  
 in zone lengths.

TITLE CONCENTRATION RATIO FOR ZONE REFINING  
 FORMAT AN(S4DP4D), NA(S4D), KC(S3DP3D3T), CK(SDP6D)  
 DATA FOF5(50)  
 SUBSCRIPTS S  
 BEGIN  
 START: KI = KEYBD  
 DELK = KEYBD  
 KMOX = KEYBD  
 AI = KEYBD  
 DELA = KEYBD  
 AMAX = KEYBD  
 NI = KEYBD  
 NMAX = KEYBD



```
FOR A = AI(DELA)AMAX BEGIN
FOR N = NI(1)NMAX BEGIN
CARR(2)
PRINT (AN) = A
CARR(2)
PRINT (NA) = N
CARR(2)
FOR K = KI(DELK)KMAX BEGIN
IF N = 1 BEGIN
Z = 1.0
GO TO ALPHA END
GO TO SUM
LOOP: TABS(2)
PRINT (KC) = K
PRINT (CK) = CRATIO
CARR(2) END END END
GO TO START

SUM: LIMS = N - 1
FOR S = 1(1) LIMS BEGIN
SUMR = 0
LIMR = S - 1
FOR R = 0(1)LIMR BEGIN
W = S - R - 1
WFAC = 1.0
RFAC = 1.0
```

```
IF W = 0
GO TO BETA
FOR I = 1(1)W
WFAC = WFAC*I
BETA: IF R = 0
GO TO EVAL
FOR I = 1(1)R
RFAC = RFAC*I
EVAL:FACRS = S↑(S - R - 2)/(WFAC*RFAC)
IF A = 0 BEGIN
IF R = 0 BEGIN
X = 1.0
GO TO CALC END
X = 0
GO TO CALC END
X = A↑R
CALC:SUMR = SUMR + FACRS*X*(R + 1 - K * A) END
FOF S[S] = K↑(S - 1)*EXP(-S*K) * SUMR END
SUMT = 0
LIMIT = N - 1
FOR T = 1(1)LIMIT BEGIN
SUMS = 0
FOR S = 1(1)T
SUMS = SUMS + FOF S[S]
SUMT = SUMT + SUMS END
```

Z = N - SUMT

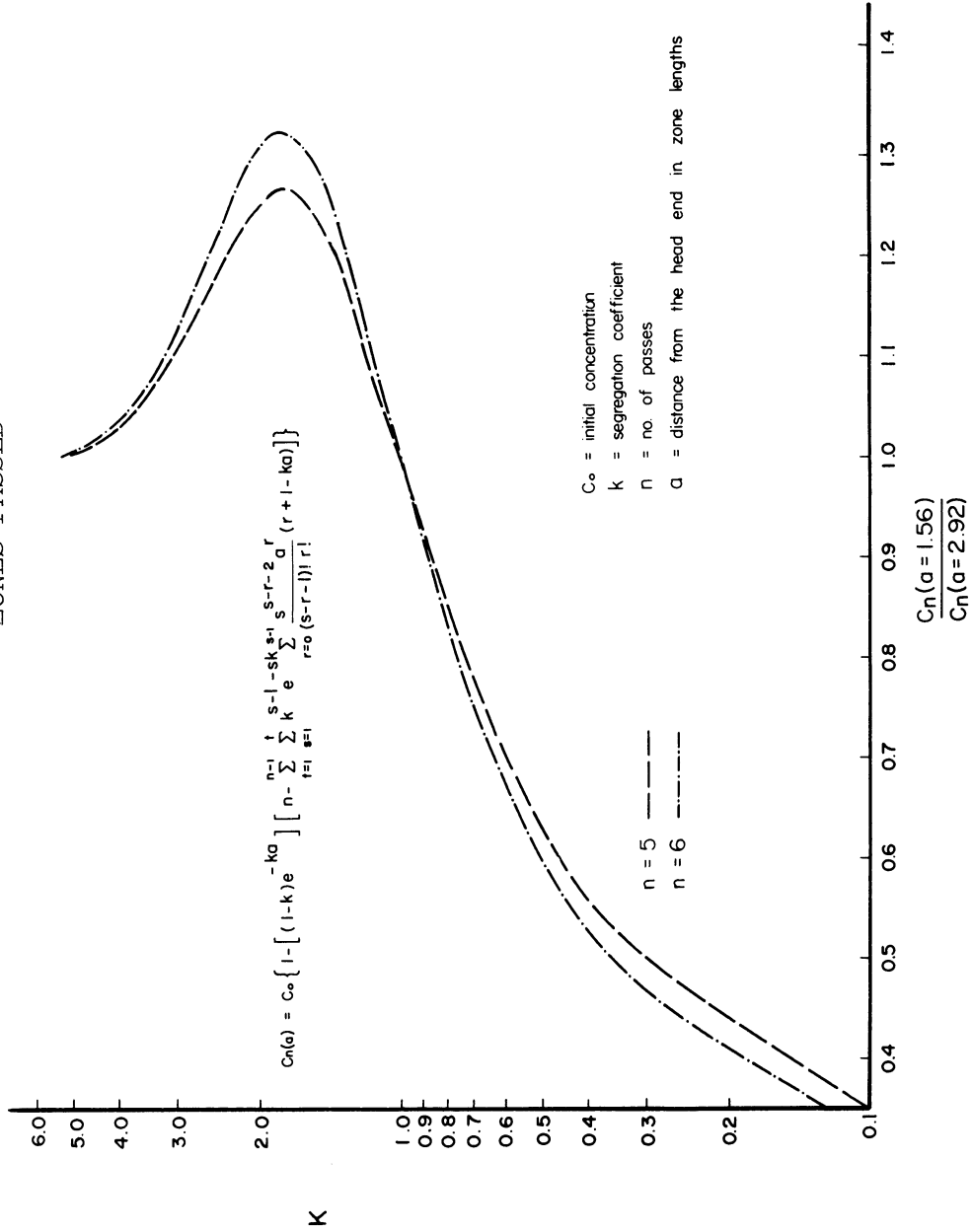
ALPHA: CRATIO = 1.0 - (1.0 - K)\*EXP(- A \* K) \* Z

GO TO LOOP

END

APPENDIX D

EFFECTIVE SEGREGATION COEFFICIENT VS. THE RATIO OF RESULTING SOLUTE CONCENTRATIONS IN THE ZONE MELTED INGOT AT 1.56 AND 2.92 ZONE LENGTHS FROM THE HEAD END FOR 5 AND 6 ZONES PASSED

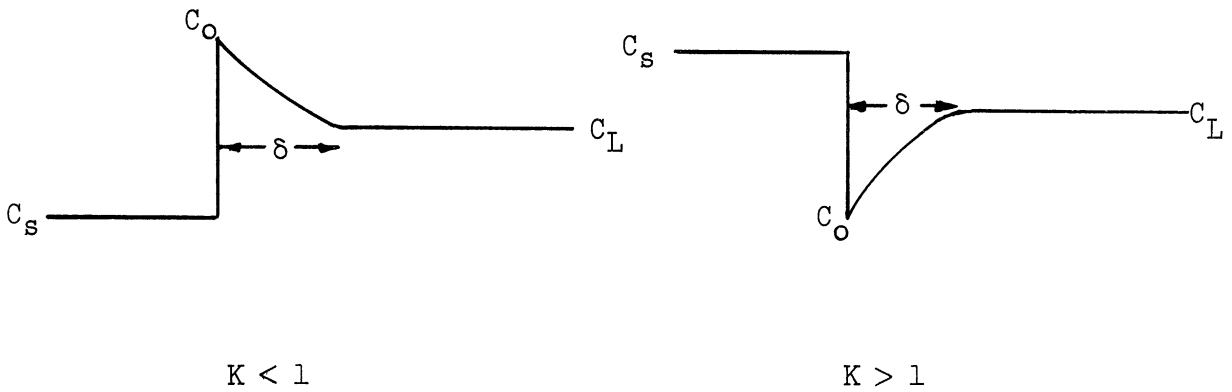


APPENDIX E

A COMPARISON OF POLYMER DIFFUSIONAL VELOCITIES  
WITH THE RATE OF ZONE TRAVEL IN ZONE MELTING A  
CYCLOHEXANE-RICH POLYSTYRENE-CYCLOHEXANE SYSTEM

$$\text{Diffusion flux, } J = -D \frac{\partial c}{\partial x} \quad (1)$$

$$\text{Diffusion velocity, } V_D = J/(\text{conc}). \quad (2)$$



$$-\frac{\partial c}{\partial x} \approx (C_o - C_L)/\delta \approx C_s \left( \frac{1}{K_{\text{equil}}} - \frac{1}{K_{\text{eff}}} \right) / \delta \quad (3)$$

where  $C_s/C_L = K_{\text{eff}}$  and  $C_s/C_o = K_{\text{equil}}$

$$\therefore V_D \approx \frac{D(\text{conc}) \left( \frac{1}{K_{\text{equil}}} - \frac{1}{K_{\text{eff}}} \right)}{\delta(\text{conc})} \quad (4)$$

$$\approx \frac{D}{\delta} \left( \frac{1}{K_{\text{equil}}} - \frac{1}{K_{\text{eff}}} \right) \quad (5)$$

Thus, a value of  $D/\delta$  is required. This can be obtained from Burton's<sup>(3)</sup> analysis, as follows:

$$\ln\left(\frac{1}{K_{\text{eff}}} - 1\right) = \ln\left(\frac{1}{K_{\text{equil}}} - 1\right) - \frac{f\delta}{D} \quad \text{for } K < 1 \quad (6)$$

$$\ln\left(1 - \frac{1}{K_{\text{eff}}}\right) = \ln\left(1 - \frac{1}{K_{\text{equil}}}\right) - \frac{f\delta}{D} \quad \text{for } K > 1 \quad (7)$$

where  $f$  is the rate of advance of the freezing interface.

For the case at hand, data are selected for the species whose molecular weight is  $1.4 \times 10^5$  ( $s^2 = 0.40 \times 10^{-24}$ ). By extrapolation of static test data, Figure 10, to 0.75 gms./100 cc., a value of  $K_{\text{equil}} = 2.60$  is obtained. From Figure 19, an effective segregation coefficient of 2.37 is obtained when  $f = 4.01$  cm./hour  $= 1.15 \times 10^{-3}$  cm./sec. From this data,  $\delta/D$  is found to be 53.9 sec./cm. Thus, by Equation (5) above,  $V_D$  is calculated to be  $0.687 \times 10^{-3}$  cm./sec. It is therefore concluded that the diffusional velocity is comparable to the rate of zone travel ( $1.15 \times 10^{-3}$  cm./sec.).

## APPENDIX F

### EXPLANATION AND PRESENTATION OF SEDIMENTATION-VELOCITY DATA FROM WHICH CONCENTRATION RATIOS IN FIGURES 10, 11, 15, 16, 17, AND 18 ARE OBTAINED

Define a sedimentation coefficient for a species  $i$  as

$$s_i = \frac{dx/dt}{\omega^2 x},$$

where  $dx/dt$  is the instantaneous rate of sedimentation at point  $x$ , the distance from the center of rotation in a centrifugal field moving with an angular velocity of  $\omega$ . It has been known for over twenty years<sup>(2,17,29)</sup> that an apparent distribution function  $g(s)$ , which gives the relative amount of a molecular species with a sedimentation coefficient  $s$ , can be obtained from refractive index gradient curves in a high centrifugal field. McCormick<sup>(17)</sup> has related the sedimentation coefficients  $s_i$  to the molecular weights  $M_i$  for a series of threadlike molecules in a  $\theta$ -solvent (such as polystyrene in cyclohexane at 35°C), and has also related the apparent distribution function  $g(s)$  to the weight fraction  $w_i$  for the same conditions. These relations are briefly outlined below.

The sedimentation coefficients have been shown<sup>(17)</sup> to be directly proportional to the square root of the molecular weight:

$$s_i = KM_i^{1/2},$$

where  $K$  is a constant. The weight fractions  $w_i$  have been shown<sup>(17)</sup> to be related to the apparent distribution functions  $g(s)$ , the sedimentation coefficients  $s_i$ , and the constant  $K$ :

$$w_i = g(s) \frac{K^2}{2s_i}.$$

It will be noted, therefore, that the weight fraction of a species with a sedimentation coefficient  $s$  can be obtained from  $g(s)$  vs.  $s$  data providing  $K$  is determined. Determination of  $K$  requires an absolute method of ascertaining the relation between  $s$  and  $M$ , which is not easily done. However, if ratios of weight fractions or of species concentrations are sufficient, it is possible simply to take the appropriate ratios of  $g(s)$ 's or of the products of  $g(s)$  times the total concentration, respectively, and thereby eliminate the need for knowing  $K$  explicitly. This approach has been followed for the work reported herein.

In the table below are values of  $g(s)$  times total sample concentration vs. the sedimentation coefficients for each of the runs whose ratios of species concentration are given in Figures 10, 11, 15, 16, 17, and 18. In addition, values of  $g(s)$  times total sample concentration vs. sedimentation coefficient are given for the amorphous, broadly distributed polystyrene as it was received.





TABLE III  
 PERCENT OF AIRFRAME DISTRIBUTION FUNCTION AND SAMPLE CONCENTRATION  $10^{-10}$  GM/CM<sup>3</sup>  
 VALIDATED GALILEO REDISTRIBUTION COEFFICIENT  
 (Refer to Table II for Explanatory Data)

Column No.	1	2	3	4	5	6	7	8	9	10	11	12	13	14	15	16	17	18	19	20	21	22	23	24	25	26	27	28	29	30	31	32	33	34	35	36	37	38	Asymptotic Sample Size for 95% Confidence	
0.1	0.05																																							0.00
0.2	0.19	0.27	0.30	0.42	0.42	0.48																																		1.44
0.3	0.28	0.59	0.71	1.10	0.67	0.67	0.26	0.41	0.30	0.41	0.18	0.23																											2.25	
0.4	0.32	1.25	0.55	1.27	0.47	0.75	0.69	1.54	0.50	0.86	0.37	0.58	0.44																										2.56	
0.5	0.29	1.89	0.48	1.51	0.54	1.10	0.56	1.99	0.26	0.64	0.22	0.44																											2.89	
0.6	0.13		0.39	1.95	0.41	1.21	0.48		0.22	0.07			0.28	0.16																									3.24	
0.7	0.08						0.17	2.08	0.05		0.10		0.18	0.49	0.25	0.60	0.22	0.31	0.53	0.74	6.44	8.04	6.50	3.44	3.72	3.96	5.72	5.72	4.93	4.13	3.68	0.37	0.36	6.32	7.20	6.68	7.55		3.72	
0.8	0.05						0.05	1.22	0.01	0.10	0.29	1.32	0.27	0.47	0.31	0.57	0.27	0.28	0.59	0.65	5.32	6.36	5.20	6.11	4.60	4.50	5.04	5.09	5.68										3.60	
0.9													0.25	0.32	0.32	0.44	0.29	0.20	0.42		4.28	4.48	4.92	5.30	4.72	4.34	5.32	5.00	4.00	3.16	2.64	0.34	0.34	4.20	4.24	4.76	4.81		3.44	
1.0													0.23	0.27	0.18	0.17		0.28		3.48	3.32	4.00			4.08	2.92	2.05	1.58											2.64	
1.1																					2.48																		2.04	
1.2																																							1.96	
1.3																																							1.12	
1.4																																							0.76	
1.5																																							0.52	
1.6																																							0.36	
1.7																																							0.16	

\* CONFIDENCE LEVEL 95%  
 GM/CM<sup>3</sup> PER

APPENDIX G

SEDIMENTATION-VELOCITY DATA FOR THE FIRST FOUR SEGMENTS OF A POLYSTYRENE-CYCLOHEXANE INGOT WITH AN INITIAL CONCENTRATION OF 2.25 gm/100 cc. ZONE MELTED WITH FIVE 6.35 cm. ZONES PASSED AT 4.83 cm/hr.

TABLE IV

EXPLANATORY DATA FOR TABLE V

Segment Location, Zone Lengths from Head End	0.20	1.56	2.92	4.28
Segment Concentra- tions gm/100 cc.	1.48	2.08	2.27	1.92
Refer to Column No.	1	2	3	4

TABLE V

PRODUCT OF APPARENT DISTRIBUTION FUNCTION AND SAMPLE CONCENTRATION  $\times 10^{-10}$  gm/100 cc. TABULATED AGAINST SEDIMENTATION COEFFICIENT  
(See Table IV for Explanatory Data)

Column No	1	2	3	4
$s \times 10^{+12}$				
0.1		0.11		
0.2		0.14		
0.3		0.34		3.58
0.4		0.78	1.86	4.15
0.5		1.35	3.97	6.53
0.6	0.01	1.87	7.33	6.22
0.7	2.09	2.87	5.20	.77
0.8	3.17	3.85	3.41	
0.9	3.31	4.20	1.01	
1.0	2.57	3.05		
1.1	2.13	2.65		
1.2	1.17	1.66		
1.3	.14	1.35		
1.4		1.15		
1.5		0.82		
1.6		0.63		
1.7		0.46		
1.8		0.22		

## BIBLIOGRAPHY

1. Almin, K. E., and Steenberg, B. "A New Approach to the Determination of Distribution Functions, Especially for Polymers," Acta Chemica Scandinavica, 11, (1957) 936-39.
2. Baldwin, R. L., and Van Holde, K. E. "Sedimentation of High Polymers," Fortschritte der Hochpolymeren-Forschung, 1, No. 4, (1960) 451-511.
3. Burton, J. A., and Schlichter, W. P. "The Distribution of Solute-Elements: Steady-State Growth," Transistor Technology, 1, D. Van Nostrand, Princeton, New Jersey (1958).
4. Cahill, J. W., and Loconti, J. D. "A Simple Polymer Fractionation Method," J. Polymer Sci., 49, (1961) S2.
5. Cantow, H. J. "Die Bestimmung der Molekulargewichts-Verteilung in der Ultrazentrifuge bei der  $\theta$ -Temperatur," Die Makromololare Chemie, 30, (1959) 169.
6. Desreux, V., and Spiegels, M. C. "Fractionation of Polythene by Extraction," Bull. Soc. Chim. Belges, 59, (1950) 476-89.
7. Eldib, I. A. "Zone Precipitation, A Separation Technique Based on Differences on Solubility, As Applied to Wax Fractionation." Separations Symposium, Petroleum Division, American Chemical Society National Meeting, St. Louis (April 1961).
8. Flory, P. J. Principles of Polymer Chemistry, Cornell University Press, Ithaca, New York (1953).
9. Flory, P. J., Garrett, R. R., Newman, S., and Mandelkern, L. "Thermodynamics of Crystallization in High Polymers," J. Polymer Sci., 12, No. 67, (1954) 97-107.
10. Fox, T. G., Jr., and Flory, P. J. "Intrinsic Viscosity Relationships for Polystyrene," J. Am. Chem. Soc., 73, (1951) 1915.
11. Guggenheim, E. A. "Statistical Thermodynamics of Mixtures with Non-Zero Energies of Mixing," Proc. Royal Soc. (London), A 183, (1944) 213.
12. Harrington, W. F., and Schachman, H. K. "Concentration Anomaly in Ultracentrifugation of Mixtures," J. Am. Chem. Soc., 75, (1953) 3533.

13. Johnston, J. P., and Ogston, A. G. "A Boundary Anomaly Found in Ultracentrifugal Sedimentation of Mixtures," Trans. Faraday Soc., 42, (1946) 789.
14. Langhammer, G. "Fractionation Effects in the Thermal Diffusion of High Polymers," Naturwissenschaften, 41 (1954) 552.
15. Lord, N. W. "Analysis of Molten-Zone Refining," Trans. AIME, 197, (1953) 1531.
16. McCormick, H. W. The Dow Chemical Company, Midland, Michigan, (Private communication).
17. McCormick, H. W. "Molecular Weight Distribution of Polystyrene by Sedimentation Velocity Analysis," J. Polymer Sci., 36, (1959) 341-49.
18. Moore, W. J. Physical Chemistry, Prentice-Hall, Englewood Cliffs, New Jersey (1955).
19. Morey, D. R., and Tamblyn, J. W. "The Determination of Molecular-Weight Distribution in High Polymers by Means of Solubility Limits," J. Applied Phys., 16, (1945) 419.
20. Nelson, E. R., Kilduff, T. J., and Benderly, A. A. "Bonding Teflon," Ind. Eng. Chem., 50, (March 1958) 329.
21. Orr, W. J. C. "The Free Energies of Solutions of Single and Multiple Molecules," Trans. Faraday Soc., 40, (1944) 320.
22. Peaker, F. W., and Robb, J. C. "A New Method of Fractionating High Polymers," Nature, 182, (1958) 1591.
23. Peaker, F. W. The Department of Chemistry, The University of Birmingham, England, (Private communication).
24. Pfann, W. G. "Principles of Zone Melting," Trans. AIME, 194, (1952) 747.
25. Pfann, W. G. Zone Melting, John Wiley and Sons, New York (1958).
26. Schultz, A. R., and Flory, P. J. "Phase Equilibria in Polymer-Solvent Systems. II. Thermodynamic Interaction Parameters from Critical Miscibility Data," J. Am. Chem. Soc., 75, (Aug. 20, 1953) 3888-92.
27. Scott, R. L. "The Thermodynamics of High Polymer Solutions: I. The Free Energy of Mixing of Solvents and Polymers of Heterogeneous Distribution," J. Chem. Phys., 13, (1945) 172-7.

28. Svedberg, T. "Zentrifugierung, Diffusion, and Sedimentation-gleichgewicht von Kolloiden und Hochmolekularen Stoffen," Kolloid Z., 36, (1925) 53.
29. Svedberg, T., and Pedersen, K. O. The Ultracentrifuge, Oxford University Press, London (1940).
30. Till, P. H., Jr. "The Growth of Single Crystals of Linear Polyethylene," J. Polymer Sci., 24, (1957) 301-306.
31. Tompa, H. Polymer Solutions, Butterworths Scientific Publications, London (1956).